



RESEARCH ARTICLE

REVISED Variable expression and silencing of CRISPR-Cas9 targeted transgenes identifies the *AAVS1* locus as not an entirely safe harbour [version 2; peer review: 2 approved, 1 not approved]

Jamie R. Bhagwan ¹, Emma Collins¹, Diogo Mosqueira¹, Mine Bakar¹, Benjamin B. Johnson¹, Alexander Thompson ¹, James G.W. Smith², Chris Denning¹

¹Department of Stem Cells, Tissue Engineering and Modelling, Centre for Biomolecular Sciences, University of Nottingham, Nottingham, NG7 2RD, UK

²Faculty of Medicine and Health Sciences, Norwich Medical School, University of East Anglia, Norwich Research Park, Norwich, NR4 7UQ, UK

v2 First published: 12 Nov 2019, 8:1911
<https://doi.org/10.12688/f1000research.19894.1>

Latest published: 10 Jul 2020, 8:1911
<https://doi.org/10.12688/f1000research.19894.2>

Abstract

Background: Diseases such as hypertrophic cardiomyopathy (HCM) can lead to severe outcomes including sudden death. The generation of human induced pluripotent stem cell (hiPSC) reporter lines can be useful for disease modelling and drug screening by providing physiologically relevant *in vitro* models of disease. The *AAVS1* locus is cited as a safe harbour that is permissive for stable transgene expression, and hence is favoured for creating gene targeted reporter lines.

Methods: We generated hiPSC reporters using a plasmid-based CRISPR/Cas9 nickase strategy. The first intron of *PPP1R12C*, the *AAVS1* locus, was targeted with constructs expressing a genetically encoded calcium indicator (R-GECO1.0) or HOXA9-T2A-mScarlet reporter under the control of a pCAG or inducible pTRE promoter, respectively. Transgene expression was compared between clones before, during and/or after directed differentiation to mesodermal lineages.

Results: Successful targeting to *AAVS1* was confirmed by PCR and sequencing. Of 24 hiPSC clones targeted with pCAG-R-GECO1.0, only 20 expressed the transgene and in these, the percentage of positive cells ranged from 0% to 99.5%. Differentiation of a subset of clones produced cardiomyocytes, wherein the percentage of cells positive for R-GECO1.0 ranged from 2.1% to 93.1%. In the highest expressing R-GECO1.0 clones, transgene silencing occurred during cardiomyocyte differentiation causing a decrease in expression from 98.93% to 1.3%. In HOXA9-T2A-mScarlet hiPSC reporter lines directed towards mesoderm lineages, doxycycline induced a peak in transgene expression after two days but this reduced by up to ten-thousand-fold over the next 8-10 days. Nevertheless, for R-GECO1.0 lines differentiated into cardiomyocytes, transgene expression was rescued by continuous puromycin drug selection, which allowed the Ca²⁺ responses associated with HCM to be investigated *in vitro* using single

Open Peer Review

Reviewer Status

	Invited Reviewers		
	1	2	3
version 2 (revision) 10 Jul 2020	 report		 report
version 1 12 Nov 2019	 report	 report	

- 1 **Carolyn Carr** , University of Oxford, Oxford, UK
- 2 **Catherine M. Verfaillie** , KU Leuven, Leuven, Belgium
Yannan Fan, KU Leuven, Leuven, Belgium
- 3 **Sara Howden**, Murdoch Children's Research Institute (MCRI), Melbourne, Australia

Any reports and responses or comments on the article can be found at the end of the article.

cell analysis.

Conclusions: Targeted knock-ins to *AAVS1* can be used to create reporter lines but variability between clones and transgene silencing requires careful attention by researchers seeking robust reporter gene expression.

Keywords

Human induced pluripotent stem cells; CRISPR/Cas9, stem-cell derived cardiomyocytes, stem-cell derived haematopoietic cells, *AAVS1* safe harbour, gene targeting, silencing

Corresponding authors: Jamie R. Bhagwan (j.bhagwan@axolbio.com), Chris Denning (chris.denning@nottingham.ac.uk)

Author roles: **Bhagwan JR:** Investigation, Visualization, Writing – Original Draft Preparation; **Collins E:** Investigation, Resources; **Mosqueira D:** Investigation, Resources, Writing – Review & Editing; **Bakar M:** Investigation, Resources; **Johnson BB:** Investigation; **Thompson A:** Conceptualization, Funding Acquisition, Supervision; **Smith JGW:** Investigation, Resources; **Denning C:** Conceptualization, Funding Acquisition, Supervision, Writing – Review & Editing

Competing interests: No competing interests were disclosed.

Grant information: This work was supported by the National Centre for the Replacement, Refinement and Reduction of Animals in Research [CRACK-IT:35911-259146, NC/K000225/1] and the Britain Israel Research and Academic Exchange Partnership [04BX14CDLG].
The funders had no role in study design, data collection and analysis, decision to publish, or preparation of the manuscript.

Copyright: © 2020 Bhagwan JR *et al.* This is an open access article distributed under the terms of the [Creative Commons Attribution License](#), which permits unrestricted use, distribution, and reproduction in any medium, provided the original work is properly cited.

How to cite this article: Bhagwan JR, Collins E, Mosqueira D *et al.* **Variable expression and silencing of CRISPR-Cas9 targeted transgenes identifies the *AAVS1* locus as not an entirely safe harbour [version 2; peer review: 2 approved, 1 not approved]** F1000Research 2020, 8 :1911 <https://doi.org/10.12688/f1000research.19894.2>

First published: 12 Nov 2019, 8:1911 <https://doi.org/10.12688/f1000research.19894.1>

REVISED Amendments from Version 1

We thank both reviewers for their constructive and helpful comments regarding the original manuscript. The amendments to the manuscript include changing the pseudocolouring of immunocytochemistry images in [Figure 2](#) and [Figure 3](#) such that R-GECO is always pseudocoloured red to aid consistency for the reader. [Figure 5](#) has also been amended to consistently display scale bars on the confocal line scan kymographs for time and laser line length.

Additional data has been included in Extended Data including original PCR genotyping of clones to detect AAVS1 integration, details of the sgRNAs and how they were designed and an alternative graphical representation of [Figure 4](#) to show DeltaCt rather than relative quantification.

More clarity was provided on the function of the HOXA9-mScarlet line, as well as the CRISPR targeting strategy to generate the isogenic sets of HCM mutant hiPSCs.

In addition, the discussion has been expanded to note a recent paper, published weeks after the original manuscript, which describes AAVS1 transgene silencing in iPSC-derived myeloid cells.

Any further responses from the reviewers can be found at the end of the article

Introduction

A key consideration for targeted gene delivery in human induced pluripotent stem cells (hiPSCs) is the genomic location at which to insert the exogenous DNA sequence to maximise transgene expression and limit disruption of critical endogenous genes and their function. To this end, a number of chromosomal locations that are amenable to integration have been exploited. These regions of the genome are commonly referred to as safe harbour loci, and often share some common properties such as limited disruption to endogenous genes, low proximity to oncogenes and a chromatin structure that is not prone to epigenetic silencing^{1,2}.

Examples of previously utilised genomic safe harbour loci include the chemokine (C-C motif) receptor 5 (*CCR5*) gene^{3,4}, the human orthologue of the mouse *Rosa26* locus (*hROSA26*)⁵, and a region within intron 2 of the Citrate Lyase Beta-Like (*CLYBL*) gene⁶.

The *AAVS1* locus is an area of chromosome 19 (position 19q13.42) that has been found to be a common integration site for exogenous DNA delivered to cultured cells with adeno-associated virus (AAV)^{7,8}. Integration into this site is associated with only limited disruption of endogenous genes. The phosphatase 1 regulatory subunit 12C (*PPP1R12C*) gene codes for a protein with a poorly defined function, and its first intron is disrupted by integration into the *AAVS1* site, with no observed deleterious consequences in targeted human pluripotent stem cells (hPSCs)^{2,9}. DNA sequences inserted at this location are supposedly protected by endogenous insulator regions¹⁰. These insulators are considered to contribute to maintaining an open chromatin conformation at the *AAVS1* locus, reducing the likelihood of transgene silencing compared to other safe harbour loci such as *CCR5*^{4,11}. However, some reports of DNA methylation dampening transgene expression in both hPSC-derived hepatocytes¹² and iPSC-derived myeloid progenitors³²

raise questions on whether a 'perfect' safe harbour locus exists. Despite this, *AAVS1* has remained popular for gene targeting^{13–16}.

We sought to utilise CRISPR/Cas9 nickase to target the *AAVS1* locus in hiPSCs and introduce a genetically encoded calcium indicator, R-GECO1.0, to enable live Ca²⁺ imaging in hiPSC-derived cardiomyocytes (hiPSC-CMs)^{18,19}. This was performed in genome engineered isogenic hiPSC lines we previously described to model the condition, hypertrophic cardiomyopathy (HCM). These included a trio of lines harbouring a *c.MYH7*^{C9123T} mutation²⁰ and a duo harbouring a *c.ACTC1*^{G301A} mutation²¹.

In addition, CRISPR Cas9 targeting of the *AAVS1* locus was used to target a doxycycline-inducible HOXA9-T2A-mScarlet cassette into hiPSCs with the aim of modulating HOXA9 during haematopoietic differentiation. HOXA9 is a transcription factor regulated spatio-temporally during haematopoietic or cardiac development²² and the aim was to examine if controlled supplemental expression of HOXA9 resulted in more efficient production of mature cells.

We found that, far from being a safe harbour locus, *AAVS1* integration associated with transgene expression that varied between clones and/or was silenced during directed differentiation towards both haematopoietic cells and cardiomyocytes. This suggests that silencing at the *AAVS1* locus is not limited to the endoderm lineage as previously described¹². Nevertheless, by altering our methods from bulk population analysis to single cell confocal laser line scan microscopy, we used the hiPSC-CMs expressing R-GECO1.0 to investigate the impact of HCM mutations on Ca²⁺ transients. Abnormalities were found in both HCM-associated mutations *c.MYH7*^{C9123T} and *c.ACTC1*^{G301A}, and this phenotype was successfully rescued with drug treatment. This demonstrates an *in vitro* alternative to some aspects of drug testing on animal models of HCM. Finally, we conclude that the *AAVS1* locus cannot be considered a true safe harbour. Researchers seeking to target this locus should check clones for transgene expression status both in hiPSCs and in differentiated progeny.

Methods

Ethical statement

Informed patient consent was obtained for all patient-derived hiPSC samples to be used for research purposes. Isolation and use of patient fibroblasts was approved by the Nottingham Research Ethics Committee (License 09/H0408/74), and sample collections are registered with the UK Clinical Research Network under project 8164.

hiPSC culture and differentiation

All cell culture experiments were performed in a type II Biological Safety Cabinet, and cells were incubated in a humidified incubator at 37°C and 5% CO₂. hiPSCs were routinely maintained in E8 medium on 1:100 Matrigel (Corning #356235) coated plastic ware (Nunc). Cells were passaged every three days by washing once with Ca²⁺/Mg²⁺-free Phosphate Buffer Saline (PBS, Gibco #14190-094), followed by incubation with TrypLE for four minutes. Subsequently, hiPSC were resuspended in E8 supplemented with 10 μM Y-27632 (ROCKi, Tocris

Bioscience #1254/10) and seeded into new Matrigel-coated flasks at approximately 20000 cells/cm². Medium was changed every day.

hiPSC differentiation to cardiomyocytes was performed as previously described^{20,21}. Briefly, culture vessels were seeded at approximately 20–40 thousand cells / cm², followed by a Matrigel™ overlay step two days later, supplemented with 1 ng/ml BMP4 [R&D #314-BP-050]. 16 hours later, medium was changed to StemPro™34- Serum Free Medium [SP34, Gibco #10639011], supplemented with 8 ng/ml Activin A (ActA, LifeTechnologies #PHC9564) and 10 ng/ml BMP4. After 48 hours medium was changed to RPMI B27 without insulin (LifeTechnologies #A1895601), with 10 μM KY0211 (R&D #4731) and 10 μM XAV939 (R&D #3748). 48 hours later, medium was changed to RPMI B27 (LifeTechnologies #0080085-SA) with 10 μM KY0211 and 10 μM XAV939. Thereafter, medium was changed every 2–3 days with fresh RPMI B27 until day 15 of differentiation, when hiPSC-CMs were dissociated using collagenase²³, re-plated, and kept in RPMI B27 for another week until phenotypic assays were performed.

hiPSC differentiation to haematopoietic cells was performed by passaging hiPSCs using Gentle Cell Dissociation Reagent (GCDR; Stem Cell Technologies #07174) and Corning cell scrapers (Sigma #CLS3008) when colonies had compacted and wells were 70–80% confluent. Differentiation was performed using STEMdiff™ Haematopoietic Kit according to the supplied protocol (Stem Cell Technologies #05310). Briefly, hiPSCs were dissociated as cell aggregates with GCDR for 7–10 minutes at room temperature, followed by scraping. Cell aggregates (50–200 μm in diameter) were seeded at different ratio densities in E8 media. The following day, only wells that contained 16–40 colonies >50 μm in diameter were selected to continue with differentiation and media was changed to Media A (day 0 of differentiation). On day two, a half Media A change was performed. On day three, media was changed to Media B and half Media B changes were performed on days five, seven and 10. On day 12, suspension cells were harvested for downstream analysis.

CRISPR-Cas9 gene targeting of the *AAVS1* locus

In order to target the *AAVS1* locus in hiPSCs, a targeting vector was constructed containing either the CAG-R-GECO1.0-IRES-Puro

cassette¹⁸ or the doxycycline-inducible HOXA9-T2A-mScarlet-CAG-G418 cassette flanked on each side with 1 kb of homology to the *AAVS1* locus²⁴. 1 μg of *AAVS1* targeting vector was transfected into 1 × 10⁶ hiPSCs, with 500 ng of each *AAVS1* guide RNA pU6 vector and 1 μg of hCas9 D10A nickase plasmid using an Amaxa 4D system (Lonza) according to the manufacturer's instruction. 24 hours after transfection, the medium was supplemented with 0.3 μg/ml puromycin (Life Technologies #A1113802) or 50 μg/ml Geneticin™ (Life Technologies #10131027) depending on the drug selection cassette for positive selection of clones up to 10 days post-transfection. Drug-resistant clones were then isolated using 0.5 mM EDTA and expanded. Clones were then genotyped using polymerase chain reaction (PCR) on genomic DNA using Phusion® polymerase (NEB Cat# M0530S) and the primers given in Table 1. PCR cycle parameters were 95°C for 2 minutes, 60–64°C for 30 seconds and 72°C for 60 seconds, with a final elongation step of 72°C for 10 minutes.

Immunocytochemistry

Dissociated hPSC-CMs or hPSCs were cultured in vitronectin-or MT-coated 96-well plates (CellCarrier, Perkin Elmer #6005550), respectively, at approximately 50K cells/cm² as described above. Cells were washed with PBS and fixed in 4% Paraformaldehyde (PFA, Sigma) at room temperature (RT) for 15 minutes. Afterwards, cells were washed in 0.1% Tween-20 (Fisher Scientific) in PBS, permeabilized with 0.1% Triton-X (Sigma) in PBS for 15 min at RT, and incubated with 4% goat serum (Sigma) in PBS (blocking solution) for one hour at RT to prevent unspecific antibody binding. Subsequently, primary antibody incubation was performed overnight at 4°C in blocking solution at the following dilutions: mouse monoclonal anti-OCT4-1:200 (Santa Cruz Biotechnology Cat# sc-5279, RRID:AB_628051), rabbit polyclonal anti-RFP-1:1000 (Abcam Cat# ab124754, RRID:AB_10971665), mouse monoclonal anti-α-actinin-1:800 (Sigma-Aldrich Cat# A7811, RRID:AB_476766). Thereafter, samples were washed three times with 0.1% Tween-20 in PBS and incubated with Alexa Fluor secondary antibodies (Life Technologies) in blocking solution for one hour at RT. Afterwards, cells were washed with 0.1% Tween-20 in PBS for 3x five minutes, followed by nuclei and/or whole cell counterstaining with 0.5 μg/ml DAPI (Sigma #D9542) or Cell Mask (1:10000, Invitrogen #H32721) in PBS, respectively, for 30 minutes at RT. Samples were

Table 1. Primers used for PCR screening of *AAVS1* integration.

PCR screen	Forward primer sequence (5' → 3')	Reverse primer sequence (5' → 3')	Annealing temperature
5' integration screen (Outside <i>AAVS1</i> Left Arm Homology – CAG promoter)	TCCCCCTCTCCGATGTTGAG	TGGGCTATGAACTAATGACCCCG	64°C
3' integration screen (IRES/Puromycin – Outside <i>AAVS1</i> Right Arm Homology)	AGCGTATTCAACAAGGGGCT	ACCCCGAAGAGTGAGTTTGCC	62°C
Biallelic targeting screen (Inside <i>AAVS1</i> Left Arm Homology – Inside <i>AAVS1</i> Right Arm Homology)	ATGCCGTCTTCACTCGCTGG	GGGGCTTTTCTGTACCAATCC	64°C

subsequently washed and stored at 4°C in PBS until automated image acquisition was performed in the Operetta™ high-content imaging system (PerkinElmer) and analysed using Harmony high-content imaging analysis software.

Live imaging mScarlet expression

HOXA9 and mScarlet expression was induced with the addition of 1 µg/ml doxycycline every 48 hours. Live imaging of mScarlet fluorescence in differentiating hiPSCs was performed using Operetta™ high-content image analysis every two days. All images were taken using a 20x objective. Brightfield images were taken using 100 ms exposure time. mScarlet imaging was performed using 400 ms exposure and an excitation wavelength of 520–550 nm and an emission wavelength of 560–630nm. Data analysis was performed using Columbus™ software (PerkinElmer) to identify and quantify cell regions expressing mScarlet fluorescence.

Gene expression analysis by qPCR

Real-time qPCR reactions were performed using TaqMan® Gene Expression Assays (Applied Biosystems) following manufacturer's instructions. Briefly, Taqman® mastermix (#4369016) including the *HOXA9* probe²⁵ was added to a MicroAmp Fast 96-well plate (#4346907). Subsequently, cDNA samples (from initial 500 ng of reverse-transcribed RNA) were added to the plate, which was thereafter sealed with a film (#4311971). Amplification was performed in ABI 7500 Real-Time PCR system (Applied Biosystems). Cycle conditions were 50°C for 2 minutes, 95°C for 10 minutes followed by 40 cycles of 95°C for 15 seconds and 60°C for 1 minute. Normalisation was performed using the housekeeping gene *B2M* or *PPIA*. Relative quantification was calculated using the $\Delta\Delta CT$ method²⁶ in Microsoft Excel.

Confocal analysis and ClampFit identification of abnormal Ca²⁺ transients

hiPSCs were differentiated as previously described^{20,21} in RPMI B27 without phenol red and dissociated on day 15 by collagenase treatment. On day 30, hiPSC-CMs were seeded at a density of 150,000 cells per well in vitronectin-N coated MatTek dishes. Intracellular Ca²⁺ transient measurements were made using an LSM 880C confocal microscope (Carl Zeiss) in the line-scan mode as previously described²⁷. CMs were located using a 40x oil objective and a longitudinal line was drawn across a single CM. The R-GECO fluorophore was excited with a 561 nm laser at 0.8% power, with a detection range of 579 – 639 nm. Line-scan images were taken every 75 milliseconds, with a pixel dwell time of 4.12 µsec, for a total of 4000 cycles resulting in a five minute scan. CMs were kept at 37°C and 5% CO₂ and allowed to spontaneously beat throughout data acquisition.

Confocal line scan images were analysed in Fiji software, a version of ImageJ (National Institute of Health). The average fluorescence intensity of each line was calculated against time to give a confocal line-scan trace. Using the 'multi kymograph' function, a corresponding kymograph image was produced. In order to calculate beat rate and arrhythmic events, data was fed into pClamp software (Molecular Devices). Baselines were adjusted to account for photobleaching

and Ca²⁺ transients were counted and analysed using the 'event detection' function. Using the event viewer, any Ca²⁺ transients that did not return to baseline and gave a 'double peak', or did not return to at least 75% of the previous Ca²⁺ transient amplitude, were considered 'abnormal', as described in 21.

Statistical analysis

All data presented as mean with standard deviation unless otherwise stated. Statistical analysis of multiple data sets was performed using GraphPad software (version 7.04).

For multiple comparisons between data sets a one-way ANOVA with Tukey's multiple comparison test was chosen. For comparing multiple data sets to a single control column, one-way ANOVA with Dunnett's multiple comparison test was chosen. Significance tests were based on p-values as follows: * p < 0.05; ** p < 0.01; *** p < 0.001; **** p < 0.0001.

Results

Knock-in of transgenes into the *AAVS1* locus

Our overarching goal was to create two isogenic sets of hiPSC lines in order to study Ca²⁺ handling in the context of *in vitro* models of the disease HCM. One isogenic trio comprised lines that were originally wild-type (*MYH7*^{WT/WT}), and then CRISPR Cas9 edited to generate heterozygous (*MYH7*^{WT/MUT}) and homozygous (*MYH7*^{MUT/MUT}) mutants for the *c.MYH7*^{C9123T} mutation²⁰. The other comprised a pair that were heterozygous originally patient-derived (*ACTC1*^{WT/MUT}) and corrected (*ACTC1*^{WT/WT}) for the *c. ACTC1*^{G301A} mutation and CRISPR Cas9 corrected (*ACTC1*^{WT/WT})^{21,28}.

The *AAVS1* locus, located within the first intron of *PPP1R12C* on chromosome 19 (Figure 1A), is a well characterised safe harbour locus². Using the five lines above, we targeted a cassette containing R-GECO1.0 reporter and a puromycin resistance cassette, driven by the CAG promoter, into the *AAVS1* locus (Figure 1A)²⁴. This was achieved by using a CRISPR-Cas9 nickase approach based on two sgRNAs. Nucleofection of the HCM-associated hiPSCs with the R-GECO1.0 construct, bidirectional sgRNAs and Cas9 D10A nickase plasmids produced puromycin-resistant clones. PCR-based screening and sequencing were used to examine the regions upstream (Figure 1B) and downstream (Figure 1C) of the insertion site, and hence identify clones that were successfully targeted in one or both alleles (Figure 2B, C).

In addition, the *MYH7*^{WT/WT} hiPSC line was used to introduce a HOXA9-T2A-mScarlet cassette driven by a doxycycline-inducible pTRE promoter into the *AAVS1* locus using the same CRISPR-Cas9 nickase approach (Figure 1A). Both 5' (Figure 1D) and 3' integration (Figure 1E) to *AAVS1* was assessed using the same PCR genotyping approach on genomic DNA to identify successfully targeted clones.

Variability in transgene expression at the *AAVS1* locus

In order to quantify R-GECO1.0 expression across the targeted clones, high content image analysis was used on hiPSCs that were dual-stained with anti-OCT4 for pluripotency and anti-RFP antibody, which identifies R-GECO1.0 (Figure 2A)²⁴.

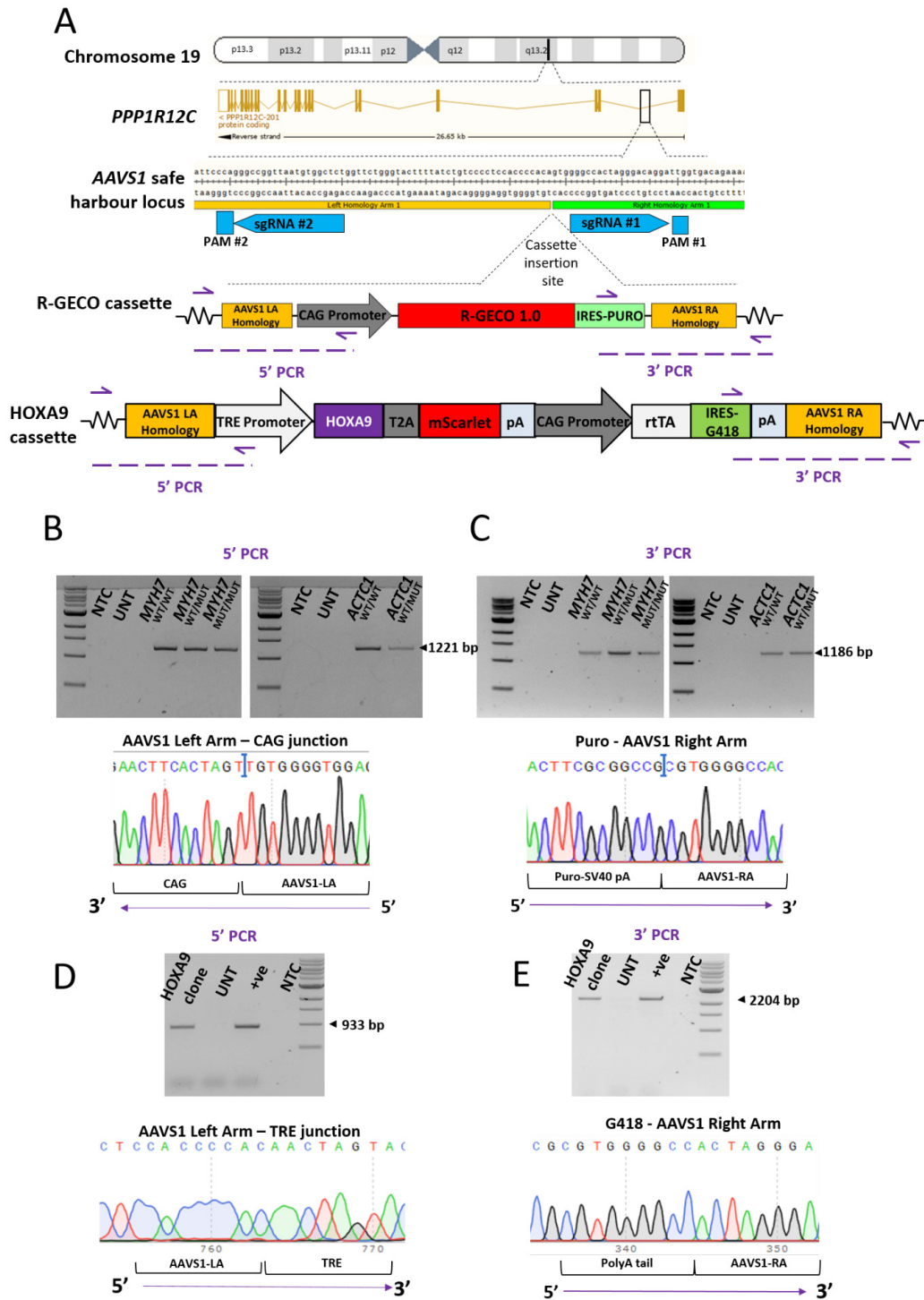


Figure 1. Generation of AAVS1-targeted hiPSC clones in an isogenic MYH7 C9123T background and an isogenic ACTC1 G301A background. (A) Schematic illustrating the chromosomal location of the AAVS1 safe harbour locus. This site was targeted using two sgRNAs in a CRISPR Cas9 nickase strategy. PAM site #1 was silently mutated (G→C) in the targeting construct to prevent it being cut by Cas9 nuclease during targeting. The inserted cassette consists of R-GECO1.0 IRES-Puromycin driven by the CAG promoter. This is flanked on each side by 1 kb of homology to the AAVS1 locus. In (B) and (C) confirmatory 5' and 3' targeting PCR screen is shown using genomic DNA isolated from the MYH7 C9123T RGECO1.0 isogenic trio (left) and the ACTC1 G301A RGECO1.0 isogenic duo (right) hiPSCs. Correct 5' targeting is indicated with a 1221bp product, with sequencing confirming the fidelity of the junction between the AAVS1 left arm homology and the start of the CAG promoter. Correct 3' targeting is indicated with an 1186bp product, with sequencing confirming the fidelity of the junction between the puromycin-SV40 pA sequence and the AAVS1 right arm homology. (D, E) Confirmatory PCR and sequencing of hiPSC clones to check 5' and 3' targeting of the AAVS1 locus with the HOXA9-T2A-mScarlet cassette.

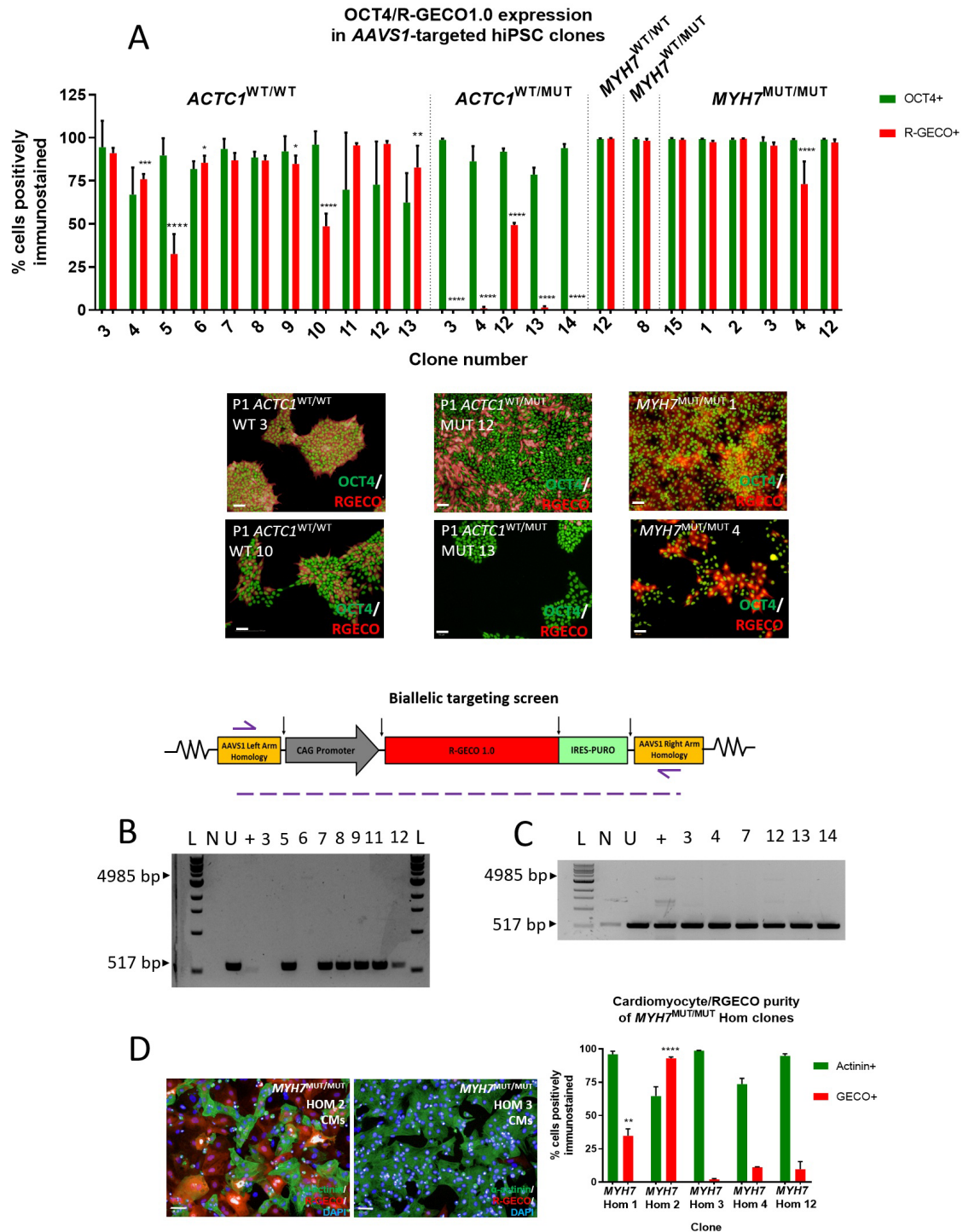


Figure 2. Immunocytochemistry-based screening of AAVS1-targeted clones showing differential expression of R-GECO1.0 between and within cell lines. (A) AAVS1 targeted hiPSC clones dual-stained for OCT4 (green) and R-GECO (red) to find the highest R-GECO-expressing clone within the five cell line genotypes. High content image analysis identified that *ACTC1*^{WT/WT} clone 3 had the highest percentage of pluripotent (94.53% OCT4+) and R-GECO (91.06% ± 1.73%) hiPSCs. *ACTC1*^{WT/MUT} clone 12 clone had the highest expression of R-GECO (49.37% ± 1.33%). Mean ± SD, n = 3 wells. One-way ANOVA with Dunnett's multiple comparison test, * p < 0.0259; ** p < 0.0045; **** p < 0.0001. Scale bars = 50 μm. (B) Biallelic targeting PCR screen on isolated gDNA from targeted *ACTC1*^{WT/WT} hiPSC clones showing homozygous clones failure to generate the 517bp PCR product. (C) Biallelic targeting PCR screen showing that all *ACTC1*^{WT/MUT} clones tested resulted in a 517bp product and were therefore heterozygous for AAVS1 targeting. L – 1kb ladder; N – no template control; U – untargeted cell line; + – AAVS1 biallelic positive control. (D) Screening *MYH7*^{MUT/MUT} clones using immunocytochemistry on differentiated hiPSC-CMs reveals a significant increase in R-GECO1.0 expression in the *MYH7*^{MUT/MUT} Hom 2 clone. Mean ± SD, n = 3 technical replicates. One-way ANOVA with Tukey's multiple comparison test, ** p < 0.006; **** p < 0.0001. Scale bars = 50 μm.

Transgene expression varied widely both between, and within, cell lines. The percentage of cells expressing R-GECO1.0 in *AAVSI*-targeted *ACTC1*^{WT/WT} hiPSC clones ranged from a maximum of 96.4% to a minimum of 32.6% (Figure 2A), and in isogenic mutant *ACTC1*^{WT/MUT} hiPSC clones from 49.4% to 0%. Selected clones for the isogenic trio of *MYH7*^{WT/WT}, *MYH7*^{WT/MUT} and *MYH7*^{MUT/MUT} hiPSCs showed comparatively high R-GECO1.0 expression exceeding 73.09% in all cases, an important requirement for a more faithful comparison between lines (Figure 2A).

This variability could not be explained by the incidence of biallelic targeting, as determined by PCR screening. Both alleles were targeted in *ACTC1*^{WT/WT} clones three and six, which exhibited high R-GECO1.0 expression as hiPSCs of 91.1% and 85.4%, respectively. This was comparable with the 95.6% and 96.4% expression observed in the monoallelically targeted clones 11 and 12, respectively (Figure 2A and 2B). Variability between clones was also seen upon differentiation, with a *MYH7*^{MUT/MUT} Hom 2 clone showing 93.1% R-GECO1.0 expression as hiPSC-CMs, significantly greater than the 2.1% expression observed in the *MYH7*^{MUT/MUT} Hom 3 clone (**** $p < 0.0001$) (Figure 2D).

Taken together, these results highlight that expression levels of transgenes seen in hiPSCs can vary significantly between *AAVSI*-targeted clones, which continued to be observed upon differentiation. Importantly, the level of variability could not be predicted and needed to be tested empirically.

Transgene silencing upon mesoderm differentiation

Three *AAVSI*-targeted clones of each *c.MYH7*^{C9123T} genotype were identified with greater than 98.3% R-GECO1.0 expression as hiPSCs (Figure 3A and 3C)²⁴. However, upon differentiation to cardiomyocytes, R-GECO1.0 expression significantly reduced in the biallelically targeted *MYH7*^{WT/WT} clone (** $p = 0.0015$). The monoallelically targeted *MYH7*^{WT/MUT} and *MYH7*^{MUT/MUT} clones experienced considerable silencing of R-GECO1.0 expression upon differentiation, with only 13.03% of *MYH7*^{WT/MUT} hiPSC-CMs and 1.33% of *MYH7*^{MUT/MUT} hiPSC-CMs expressing R-GECO1.0 (**** $p < 0.0001$) (Figure 3A–C). Nevertheless, to enhance the utility of these lines, particularly the low expressing *MYH7*^{MUT/MUT} clone, puromycin enrichment of the hiPSCs over three passages was used to significantly increase the number of R-GECO1.0 expressing hiPSC-CMs from 1.3% to 18.9% (** $p = 0.0003$) (Figure 3D). These results show that high transgene expression from the *AAVSI* locus as hiPSCs is not a guarantee of continued high expression upon differentiation, and points towards some extent of silencing upon cardiac differentiation.

Next, we sought to investigate the time at which silencing occurs during differentiation. To do this, we used the *AAVSI*-targeted doxycycline-inducible HOXA9-T2A-mScarlet line and differentiated the hiPSCs towards either cardiomyocyte or haematopoietic fate. As expected, the addition of 1 µg/ml doxycycline every 48 hours induced expression of *HOXA9*

and mScarlet during directed cardiac and haematopoietic differentiation. qRT-PCR analysis of *HOXA9* expression showed an increase of 22738-fold higher expression compared to untargeted hiPSC control on day 0 of cardiomyocyte differentiation (Figure 4A)²⁴. However, *HOXA9* expression decreased thereafter so that by day 10, expression levels were only 175-fold greater than untargeted hiPSC control. Similarly, qRT-PCR analysis during haematopoietic differentiation revealed peak expression of *HOXA9* occurring on day two, with 45666-fold greater expression than untargeted hiPSC control, decreasing thereafter to 64-fold expression on day 12 (Figure 4D). These results were mirrored at the protein level, where early peak expression of mScarlet fluorescence occurred on day 0 of cardiomyocyte differentiation (Figure 4B and 4C) and on day two of haematopoietic differentiation (Figure 4E and 4F), decreasing at later timepoints of differentiation.

For the haematopoietic differentiation, expression of the key mesoderm markers *MIXL1* and Brachyury peaked on day two (Figure 4G and 4H). This suggests that silencing of the *AAVSI* locus can occur immediately after mesoderm patterning. As a whole, these results show a progressive silencing of transgene expression as mesoderm differentiation progresses.

AAVSI-targeted R-GECO1.0 expressing clones as a tool for *in vitro* disease modelling and drug screening

Despite some obstacles due to unanticipated *AAVSI* silencing, isogenic R-GECO1.0 expressing clones in genetic backgrounds associated with HCM were successfully generated and used to image Ca²⁺ transients using confocal laser line scan microscopy. As this technique involves assaying single cells, even poorly expressing clones were useful. By monitoring the fluctuation of R-GECO1.0 fluorescence over time, Ca²⁺ transient traces could be generated for each line (Figure 5A–C and 5E–F)²⁴. Despite some expected variability in spontaneous beat rate between wild-type hiPSC-CMs (Figure 5A and 5E)²⁹, for both the *c.MYH7*^{C9123T} and *c.ACTC1*^{G301A} mutations, increasing mutation load resulted in an increased incidence of abnormal Ca²⁺ transient events. *MYH7*^{WT/WT} hiPSC-CMs only presented 1.1% aberrant Ca²⁺ transient events, increasing to 4.33% in *MYH7*^{WT/MUT} hiPSC-CMs, and further increasing to 11.2% in *MYH7*^{MUT/MUT} hiPSC-CMs ($p < 0.0001$) (Figure 5D). This represented a ten-fold increase in the occurrence of aberrant Ca²⁺ transients in the homozygous mutant compared to isogenic wild-type control. Likewise, 15.65% of Ca²⁺ transients in *ACTC1*^{WT/MUT} hiPSC-CMs were calculated as being aberrant, compared to 6.7% ($\pm 0.6\%$) in *ACTC1*^{WT/WT} isogenic control hiPSC-CMs ($p = 0.0118$) (Figure 5G). This demonstrated the utility of the *AAVSI*-targeted R-GECO1.0 cell lines for *in vitro* disease modelling and phenotyping as a credible alternative to the use of animal models.

We then attempted to rescue the aberrant Ca²⁺ transient phenotype in our HCM models with the use of a combination treatment of ranolazine, a late sodium channel blocker, and dantrolene, a ryanodine receptor antagonist. In combination at 10 µM with 24 hours incubation, these two drugs significantly

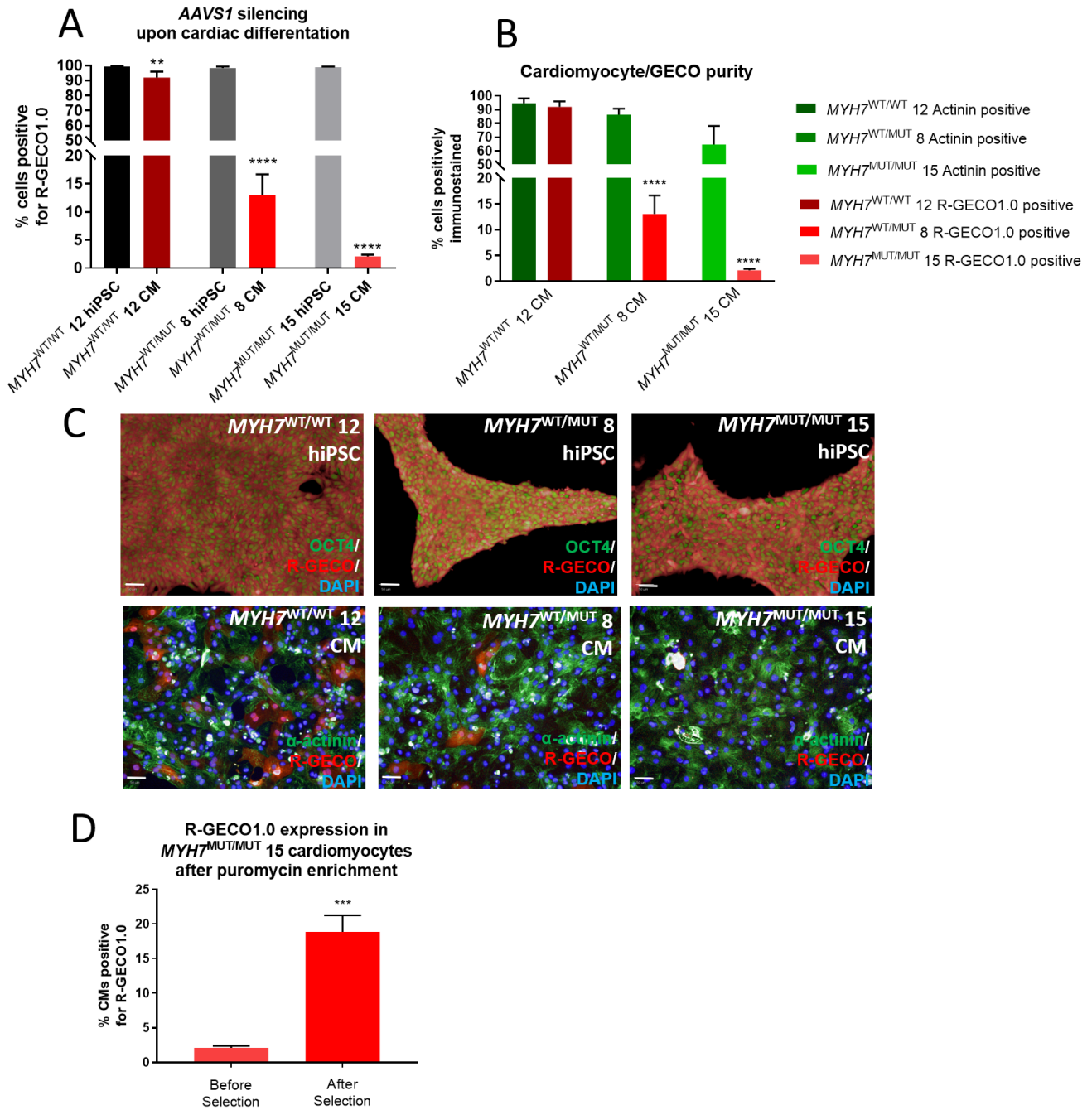


Figure 3. Changes in transgene expression during differentiation and antibiotic selection. (A) Immunocytochemistry using an anti-RFP antibody to detect R-GECO1.0 expression shows a reduction in signal in MYH7^{WT/MUT} 8 and MYH7^{MUT/MUT} 15 cell lines upon differentiation from hiPSCs to hiPSC-CMs. Mean \pm SD, n = 3 technical replicates. One-way ANOVA with Sidak's multiple comparison test, ** p = 0.0015; **** p \leq 0.0001. (B) Percentage purity data for cardiomyocytes determined by alpha-actinin staining (green), for R-GECO1.0 by RFP staining (red). Mean \pm SD, n = 3 technical replicates. One-way ANOVA with Sidak's multiple comparison test, **** p \leq 0.0001. (C) Targeted hiPSC lines show variations in expression of R-GECO1.0 protein upon differentiation. hiPSC lines, identified by OCT4 staining (green, top row) show high R-GECO1.0 expression (red). Upon differentiation to cardiomyocytes, identified by α -actinin staining (green, bottom row), MYH7^{WT/MUT} 8 and MYH7^{MUT/MUT} 15 hiPSC-CMs show lower R-GECO1.0 expression (red). Scale bars = 50 μ m. (D) R-GECO1.0 expression in MYH7^{MUT/MUT} 15 cardiomyocytes is significantly improved with three passages of hiPSC cell culture in 0.3 μ g/ml puromycin and differentiation carried out in media supplemented with puromycin. Mean \pm SD, n = 3 technical replicates. Unpaired t-test, *** p = 0.0003.

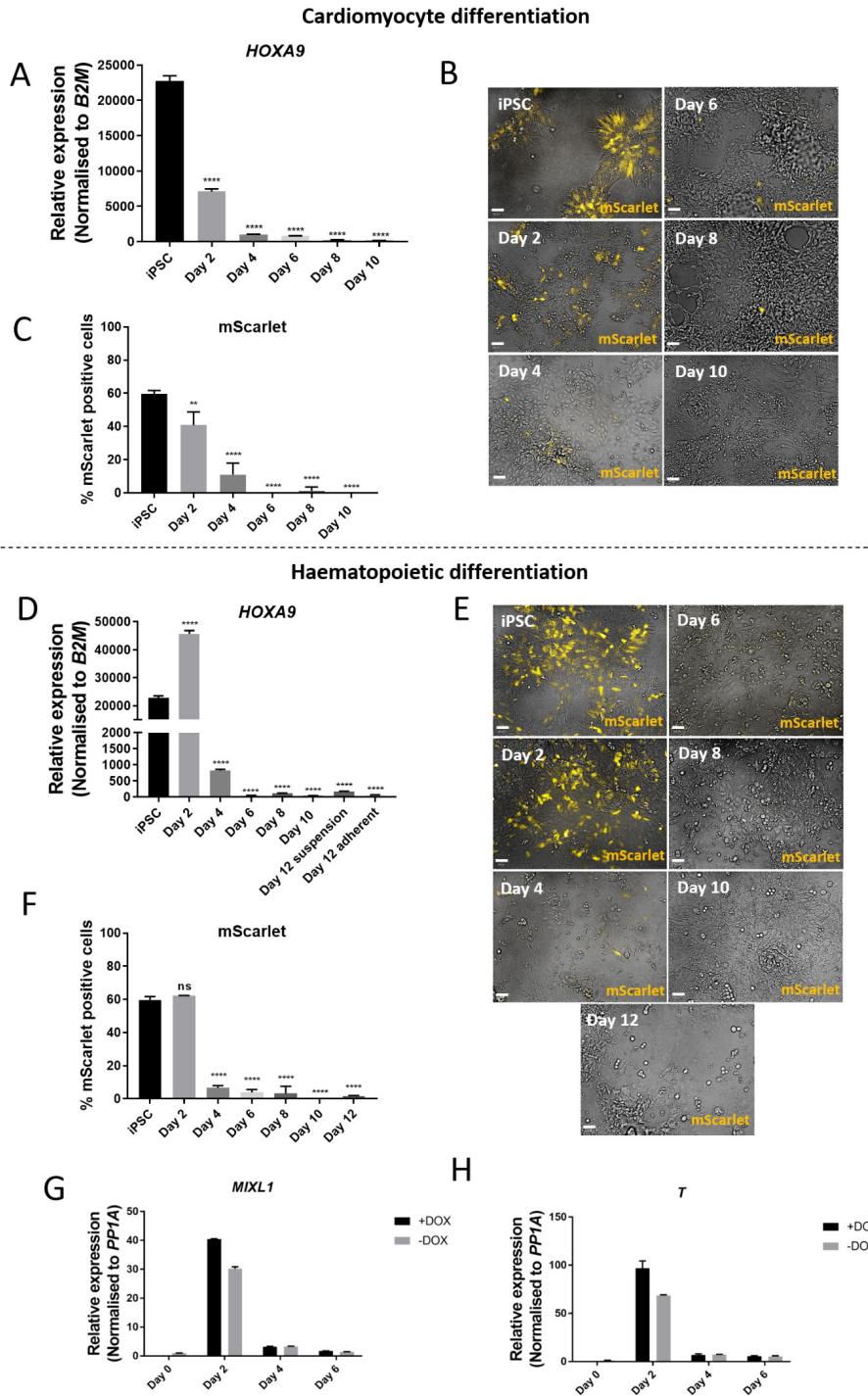


Figure 4. Differentiation towards cardiomyocytes or haematopoietic cells results in silencing of AAVS1-targeted transgene after mesoderm induction. (A) qRT-PCR performed on hiPSCs targeted at the *AAVS1* locus with a doxycycline-inducible HOXA9-T2A-mScarlet construct undergoing cardiomyocyte differentiation. Relative expression to untargeted hiPSCs. Reduced expression of the transgene is observed from day two onwards. (B) Live imaging of AAVS1-targeted hiPSCs undergoing cardiomyocyte differentiation at different timepoints. mScarlet expression peaks on day 0 and reduces throughout the differentiation, despite repeated doxycycline treatment. Scale bars = 50 μ m. (C) Quantification of mScarlet expression using high content image analysis at different timepoints during cardiomyocyte differentiation. (D) qRT-PCR performed on hiPSCs targeted at the *AAVS1* locus with a doxycycline-inducible HOXA9-T2A-mScarlet construct undergoing haematopoietic differentiation. Relative expression to untargeted hiPSCs. Reduced expression of the transgene is observed from day four onwards. (E) Live imaging of AAVS1-targeted hiPSCs undergoing haematopoietic differentiation at different timepoints. Scale bars = 50 μ m. (F) Quantification of mScarlet expression using high content image analysis shows peak expression on day two and reduced expression thereafter. Mean \pm SD, n = 2 differentiations. One-way ANOVA with Dunnett's multiple comparison test, ** p = 0.0036; **** p \leq 0.0001. (G, H) The mesoderm markers *MIXL1* and Brachyury (*T*) show peak expression at day two of haematopoietic differentiation.

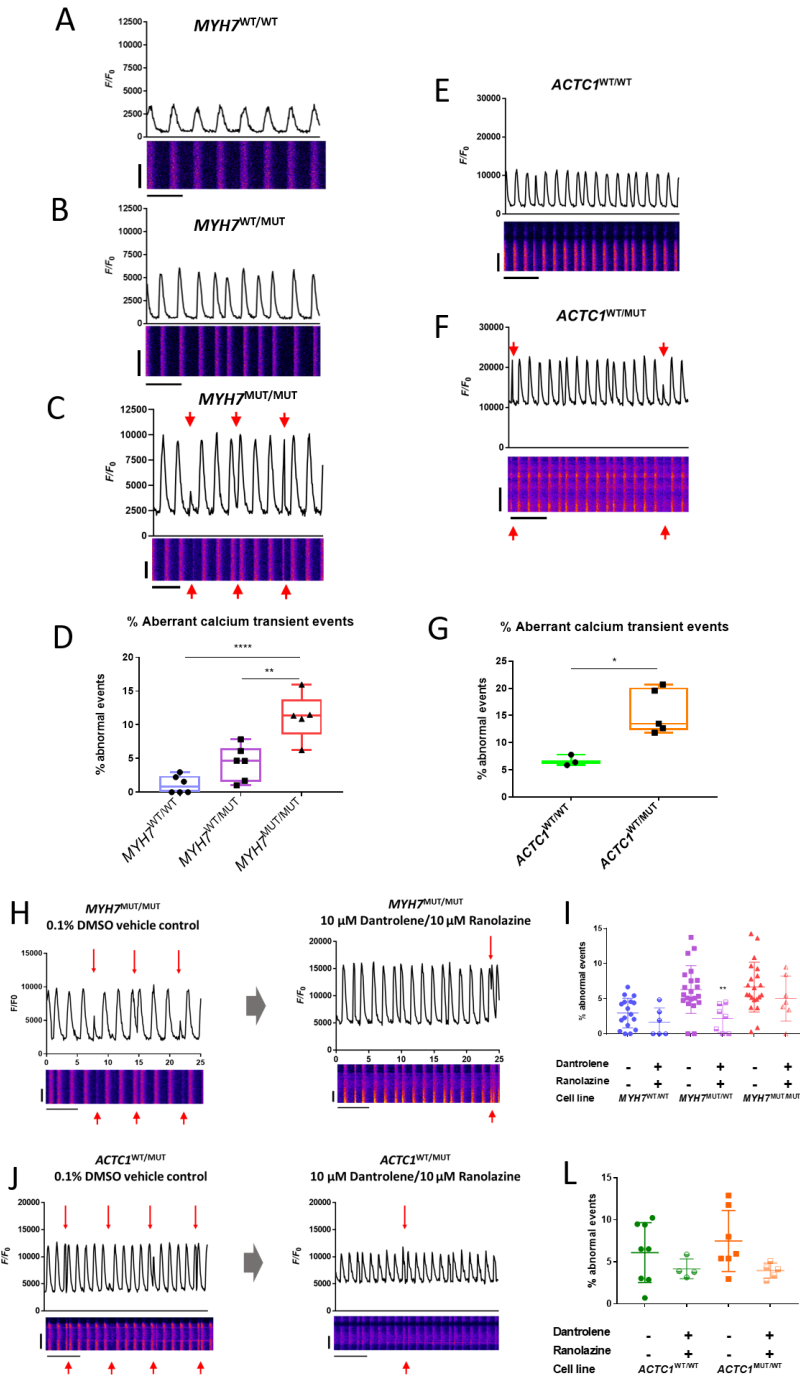


Figure 5. Functional application of AAVS1-targeted R-GECO1.0 expressing clones for *in vitro* disease modelling of HCM and phenotypic rescue with drug treatment. (A–C) Representative 25-second confocal laser line scan traces and kymographs for isogenic trio of *c.MYH7*^{G39123T} R-GECO1.0 expressing hiPSC-CMs at day 30. Abnormal Ca²⁺ transient events (red arrows) increase in frequency with mutation load. x-axis scale bar = 20 μm, y-axis scale bar = 5 seconds. (D) Ca²⁺ transient event detection and quantification showing percentage of Ca²⁺ transients deemed abnormal. Data presented as mean ±SD, n = 6 scans across three differentiations. Kruskal-Wallis test with Dunn’s multiple comparison test; ** p = 0.0018, **** p < 0.0001. (E–F) Representative 25-second confocal laser line scan traces and kymographs for isogenic pair of *c.ACTC1*^{G301A} R-GECO1.0 expressing hiPSC-CMs at day 30. Abnormal Ca²⁺ transient events (red arrows) increase in frequency with mutation load. x-axis scale bar = 20 μm, y-axis scale bar = 5 seconds. (G) Box-plot showing % of total Ca²⁺ transient events detected deemed abnormal by event detection software. Data presented as mean ±SD, n = 5 scans from three differentiations. Unpaired t-test; * p = 0.0118. (H–L) Representative line scans and event detection quantification showing a reduction in abnormal Ca²⁺ transient events upon treatment with 10 μM ranolazine and 10 μM dantrolene compared to 0.1% DMSO vehicle control. Data presented as mean ±SD, n > 4 cells across minimum of two differentiations. Kruskal-Wallis test with Dunn’s multiple comparison test; ** p = 0.0068. x-axis scale bar = 20 μm, y-axis scale bar = 5 seconds.

reduced the frequency of aberrant Ca²⁺ transient events in *MYH7* mutant hiPSC-CMs. In *MYH7*^{WT/MUT} hiPSC-CMs aberrant Ca²⁺ transient event frequency was reduced from 6.32% (±3.4%) in vehicle control to 2.18% (±1.9%) with drug treatment (p = 0.0068) (Figure 5H–I).

These results show that abnormalities in Ca²⁺ transients caused by the sarcomeric mutations *c.MYH7*^{C9123T} or *c.ACTC1*^{G301A} can be identified with *AAVSI*-targeted R-GECO1.0 expression, and this phenotype can be subsequently rescued with targeted pharmacological intervention aimed at reducing intracellular Na⁺ and Ca²⁺.

Discussion

Precise integration of exogenous DNA into the genome is often performed by targeting a genomic ‘safe harbour’ locus that can tolerate gene insertion with few deleterious effects and limited transgene silencing. The *AAVSI* locus is a popular choice for targeted knock in of exogenous DNA^{16,17}. This region of the genome is claimed to facilitate robust and persistent transgene expression¹¹, aided by flanking insulator regions¹⁰. Here, we show variable success targeting the *AAVSI* locus with the genetically encoded calcium indicator R-GECO1.0 or a doxycycline-inducible HOXA9-T2A-mScarlet cassette using a CRISPR Cas9 nickase approach.

Variability in R-GECO1.0 expression between *AAVSI*-targeted clones as hiPSCs was observed, highlighting the importance of thorough screening of clones. Unsurprisingly, clones that had undergone biallelic targeting retained high R-GECO1.0 expression as hiPSCs, yet monoallelically targeted clones ranged from high expression to significantly reduced R-GECO1.0 expression. These incidences of low expression as hiPSCs may be due to clone-specific silencing, or some clones favouring expression from the untargeted allele. It has been shown that some genes within cells favour monoallelic expression³⁰. Indeed, our own studies using an antibody for the *c.ACTC1*^{G301A} mutation have shown that cells heterozygous for the mutation only express mutant protein in ~50% of the population²¹. These results highlight the heterogeneity that can exist between clones once they have been generated.

Even with the identification of *AAVSI*-targeted clones that exhibited robust R-GECO1.0 expression, there were instances of silencing upon differentiation to hiPSC-CMs. Transgene silencing at the *AAVSI* locus has previously been shown upon differentiation towards hepatocyte-like cells, with *de novo* methylation of the locus found to be responsible¹². However, the aforementioned report claims that this silencing effect is restricted to endoderm differentiations. With the use of the *AAVSI*-targeted HOXA9-T2A-mScarlet cell line, we show that in two mesoderm-specific differentiations towards cardiomyocytes and haematopoietic cells, silencing of expression occurs immediately after mesoderm specification and peak expression of *MIXL1* and *Brachyury*. This is in agreement with a recent report which demonstrated differential transgene methylation in *AAVSI*-targeted iPSC-derived myeloid cells¹³. We therefore postulate that *AAVSI*-mediated silencing, likely

as a result of *de novo* methylation, can occur upon differentiation to various germ layers, and therefore *AAVSI* cannot be considered a true safe harbour locus.

The choice of promoter may also play a role in *AAVSI*-mediated silencing, as a previous report has shown *AAVSI* silencing of eGFP expression when using the EF1a promoter that was overcome with the use of the stronger CAG promoter³¹. This influenced our decision to opt for the CAG promoter over the EF1a promoter in our constructs. Indeed, the CAG promoter appears to exhibit some insulation from methylation of transgenes at the *AAVSI* locus¹². In addition, a recent report elegantly demonstrated that contextual silencing at the *AAVSI* locus of iPSC-derived myeloid precursors can occur with varying efficiency depending on the chosen promoter¹³.

When attempting to express two separate transgenes from the same cassette at the *AAVSI* locus, the choice of peptide cleavage sequence is also important. We observed inefficient peptide cleavage when using the P2A sequence, as determined by Western Blot (see *Extended data*)²⁴. This informed our choice of using the T2A or IRES sequences for translation of multicistronic cassettes in subsequent targeting constructs. It has been claimed that the P2A cleavage sequence is the most efficient self-cleaving peptide, followed by T2A and E2A, when used to cleave a bicistronic vector in three different human cell lines, including HeLa³². We cannot reconcile this with our data, as co-expression of multicistronic cassette elements from the *AAVSI* locus in hiPSCs has been achieved using the IRES and T2A sequence, but not the P2A sequence.

Depending on the application of the targeted cell lines, some *AAVSI*-mediated silencing can be tolerated. For the R-GECO1.0 expressing lines, maintaining puromycin selection and using a single cell confocal laser line scan assay to study Ca²⁺ transients meant that abnormalities in Ca²⁺ handling could be identified in cell lines harbouring the *c.MYH7*^{C9123T} or *c.ACTC1*^{G301A} mutations. This represents an *in vitro* model of HCM that can offer an alternative to the use of animal models. Furthermore, this phenotype could be rescued with combination treatment with dantrolene and ranolazine^{20,21}. However, the aim with the doxycycline-inducible HOXA9-T2A-mScarlet cell line was to modulate HOXA9 expression at different time-points throughout haematopoietic differentiation. Clearly, the clone described herein is not suitable for this task.

In conclusion, one must carefully select *AAVSI*-targeted clones depending on their application due to the risk of transgene silencing upon differentiation. Other potential safe harbour loci, such as *CLYBL*, have been claimed to deliver five- to ten-fold higher fluorescent transgene expression than *AAVSI*⁶. However, as silencing cannot be predicted, multiple clones must be thoroughly checked for expression level and chosen according to their application. Our results dispute the claims of robust and persistent transgene expression from *AAVSI*¹¹, and complements reports that show silencing at *AAVSI* upon differentiation to endoderm lineage¹², by showing similar silencing upon mesoderm differentiation.

Data availability

Underlying data

FigShare: Variable expression and silencing of CRISPR-Cas9 targeted transgenes identifies the AAVS1 locus as not an entirely safe harbour. <https://doi.org/10.6084/m9.figshare.c.4573316.v3>²⁴

This project contains the following underlying data:

- Figure 1 – data (raw PCR integration gel images in TIF format; and sequencing chromatograms underlying Figure 1 as AB1 files)
- Figure 2 – data (raw immunocytochemistry images in PNG format; PCR gel images in TIF and PNG format; and XLS files containing immunocytochemistry expression quantification data underlying Figure 2)
- Figure 3 – data (raw immunocytochemistry images in PNG format; and XLS files containing expression quantification data underlying Figure 3)
- Figure 4 – data (raw live imaging images in PNG format; XLS files containing qPCR data underlying Figure 4)
- Figure 4 data – Raw qPCR data (XLS files containing raw qPCR data)
- Figure 5 – data (kymographs in PNG format; XLS files containing raw confocal laser line scan data underlying Figure 5)
- Figure 7 – data (raw PCR integration gel images in TIF format)

Extended data

FigShare: Variable expression and silencing of CRISPR-Cas9 targeted transgenes identifies the AAVS1 locus as not an

entirely safe harbour. <https://doi.org/10.6084/m9.figshare.c.4573316.v3>²⁴

This project contains the following extended data:

- Figure 6. Western Blot to show incomplete cleavage of multicistronic cassette when using the P2A peptide cleavage sequence (TIF image file)
- Figure 7. PCR screening of hiPSC clones to check for AAVS1 integration (TIF image file)
- Figure 8. sgRNA design (TIF image file)
- Table 2.1. Guide 2 off-target locations (XLS file)
- Table 2.2 Guide 3 off-target locations (XLS file)
- Figure 9. Delta Ct representation of HOXA9 expression in AAVS1-targeted hiPSCs (TIF image file)
- Protocol for CRISPR Cas9 knock-in at the AAVS1 locus and subsequent screening (a step-by-step procedure for performing CRISPR Cas9 knock-in at the AAVS1 locus of hiPSCs, followed by subsequent screening techniques in DOCX format)

Data are available under the terms of the [Creative Commons Attribution 4.0 International license](https://creativecommons.org/licenses/by/4.0/) (CC-BY 4.0).

Acknowledgements

The original Myc-P2A-R-GECO1.0 construct plasmid was received as a kind gift from Dr Matt Daniels at The University of Manchester¹⁷. hCas9_D10A was a gift from Professor George Church (Addgene plasmid #41816).

References

1. Papapetrou EP, Schambach A: **Gene Insertion Into Genomic Safe Harbors for Human Gene Therapy.** *Mol Ther.* 2016; **24**(4): 678–84. [PubMed Abstract](#) | [Publisher Full Text](#) | [Free Full Text](#)
2. Sadelain M, Papapetrou EP, Bushman FD: **Safe harbours for the integration of new DNA in the human genome.** *Nat Rev Cancer.* 2011; **12**(1): 51–8. [PubMed Abstract](#) | [Publisher Full Text](#)
3. Lombardo A, Genovese P, Beausejour CM, *et al.*: **Gene editing in human stem cells using zinc finger nucleases and integrase-defective lentiviral vector delivery.** *Nat Biotechnol.* 2007; **25**(11): 1298–306. [PubMed Abstract](#) | [Publisher Full Text](#)
4. van Rensburg R, Beyer I, Yao XY, *et al.*: **Chromatin structure of two genomic sites for targeted transgene integration in induced pluripotent stem cells and hematopoietic stem cells.** *Gene Ther.* 2013; **20**(2): 201–14. [PubMed Abstract](#) | [Publisher Full Text](#) | [Free Full Text](#)
5. Irion S, Luche H, Gadue P, *et al.*: **Identification and targeting of the ROSA26 locus in human embryonic stem cells.** *Nat Biotechnol.* 2007; **25**(12): 1477–82. [PubMed Abstract](#) | [Publisher Full Text](#)
6. Cerbini T, Funahashi R, Luo Y, *et al.*: **Transcription activator-like effector nuclease (TALEN)-mediated CLYBL targeting enables enhanced transgene expression and one-step generation of dual reporter human induced pluripotent stem cell (iPSC) and neural stem cell (NSC) lines.** *PLoS One.* 2015; **10**(1): e0116032. [PubMed Abstract](#) | [Publisher Full Text](#) | [Free Full Text](#)
7. Samulski RJ, Zhu X, Xiao X, *et al.*: **Targeted integration of adeno-associated virus (AAV) into human chromosome 19.** *EMBO J.* 1991; **10**(12): 3941–50. [PubMed Abstract](#) | [Publisher Full Text](#) | [Free Full Text](#)
8. Heister T, Heid I, Ackermann M, *et al.*: **Herpes simplex virus type 1/adeno-associated virus hybrid vectors mediate site-specific integration at the adeno-associated virus preintegration site, AAVS1, on human chromosome 19.** *J Virol.* 2002; **76**(14): 7163–73. [PubMed Abstract](#) | [Publisher Full Text](#) | [Free Full Text](#)
9. Hockemeyer D, Soldner F, Beard C, *et al.*: **Efficient targeting of expressed and silent genes in human ESCs and iPSCs using zinc-finger nucleases.** *Nat Biotechnol.* 2009; **27**(9): 851–7. [PubMed Abstract](#) | [Publisher Full Text](#) | [Free Full Text](#)
10. Ogata T, Kozuka T, Kanda T: **Identification of an insulator in AAVS1, a preferred region for integration of adeno-associated virus DNA.** *J Virol.* 2003; **77**(16): 9000–7. [PubMed Abstract](#) | [Publisher Full Text](#) | [Free Full Text](#)
11. Smith JR, Maguire S, Davis LA, *et al.*: **Robust, persistent transgene expression in human embryonic stem cells is achieved with AAVS1-targeted integration.** *Stem Cells.* 2008; **26**(2): 496–504. [PubMed Abstract](#) | [Publisher Full Text](#)

12. Ordovás L, Boon R, Pistoni M, *et al.*: **Efficient Recombinase-Mediated Cassette Exchange in hPSCs to Study the Hepatocyte Lineage Reveals AAVS1 Locus-Mediated Transgene Inhibition.** *Stem Cell Reports.* 2015; 5(5): 918–31.
[PubMed Abstract](#) | [Publisher Full Text](#) | [Free Full Text](#)
13. Klatt D, Cheng E, Hoffmann D, *et al.*: **Differential Transgene Silencing of Myeloid-Specific Promoters in the AAVS1 Safe Harbor Locus of Induced Pluripotent Stem Cell-Derived Myeloid Cells.** *Hum Gene Ther.* 2020; 31(3–4): 199–210.
[PubMed Abstract](#) | [Publisher Full Text](#) | [Free Full Text](#)
14. Wang J, DeClercq JJ, Hayward SB, *et al.*: **Highly efficient homology-driven genome editing in human T cells by combining zinc-finger nuclease mRNA and AAV6 donor delivery.** *Nucleic Acids Res.* 2016; 44(3): e30.
[PubMed Abstract](#) | [Publisher Full Text](#) | [Free Full Text](#)
15. Lombardo A, Cesana D, Genovese P, *et al.*: **Site-specific integration and tailoring of cassette design for sustainable gene transfer.** *Nat Methods.* 2011; 8(10): 861–9.
[PubMed Abstract](#) | [Publisher Full Text](#)
16. Yada RC, Ostrominski JW, Tunc I, *et al.*: **CRISPR/Cas9-Based Safe-Harbor Gene Editing in Rhesus iPSCs.** *Curr Protoc Stem Cell Biol.* 2017; 43: 5A.11.1–5A.11.14.
[PubMed Abstract](#) | [Publisher Full Text](#) | [Free Full Text](#)
17. Castaño J, Bueno C, Jiménez-Delgado S, *et al.*: **Generation and characterization of a human iPSC cell line expressing inducible Cas9 in the “safe harbor” AAVS1 locus.** *Stem Cell Res.* 2017; 21: 137–140.
[PubMed Abstract](#) | [Publisher Full Text](#) | [Free Full Text](#)
18. Chang YF, Broyles CN, Brook FA, *et al.*: **Non-invasive phenotyping and drug testing in single cardiomyocytes or beta-cells by calcium imaging and optogenetics.** *PLoS One.* 2017; 12(4): e0174181.
[PubMed Abstract](#) | [Publisher Full Text](#) | [Free Full Text](#)
19. Sparrow AJ, Sievert K, Patel S, *et al.*: **Measurement of Myofilament-Localized Calcium Dynamics in Adult Cardiomyocytes and the Effect of Hypertrophic Cardiomyopathy Mutations.** *Circ Res.* 2019; 124(8): 1228–1239.
[PubMed Abstract](#) | [Publisher Full Text](#) | [Free Full Text](#)
20. Mosqueira D, Mannhardt I, Bhagwan JR, *et al.*: **CRISPR/Cas9 editing in human pluripotent stem cell-cardiomyocytes highlights arrhythmias, hypocontractility, and energy depletion as potential therapeutic targets for hypertrophic cardiomyopathy.** *Eur Heart J.* 2018; 39(43): 3879–3892.
[PubMed Abstract](#) | [Publisher Full Text](#) | [Free Full Text](#)
21. Smith JGW, Owen T, Bhagwan JR, *et al.*: **Isogenic Pairs of hiPSC-CMs with Hypertrophic Cardiomyopathy/LVNC-Associated ACTC1 E99K Mutation Unveil Differential Functional Deficits.** *Stem Cell Reports.* 2018; 11(5): 1226–1243.
[PubMed Abstract](#) | [Publisher Full Text](#) | [Free Full Text](#)
22. Behrens AN, Iacovino M, Lohr JL, *et al.*: **Nkx2-5 mediates differential cardiac differentiation through interaction with Hoxa10.** *Stem Cells Dev.* 2013; 22(15): 2211–2220.
[PubMed Abstract](#) | [Publisher Full Text](#) | [Free Full Text](#)
23. Breckwoldt K, Letuffe-Brenière D, Mannhardt I, *et al.*: **Differentiation of cardiomyocytes and generation of human engineered heart tissue.** *Nat Protoc.* 2017; 12(6): 1177–1197.
[PubMed Abstract](#) | [Publisher Full Text](#)
24. Bhagwan J, Collins E, Mosqueira D, *et al.*: **Variable expression and silencing of CRISPR-Cas9 targeted transgenes identifies the AAVS1 locus as not an entirely safe harbour.** *figshare.* Collection. 2019.
<http://www.doi.org/10.6084/m9.figshare.c.4573316.v3>
25. Dickson GJ, Lappin TR, Thompson A: **Complete array of HOX gene expression by RQ-PCR.** *Methods Mol Biol.* 2009; 538: 369–93.
[PubMed Abstract](#) | [Publisher Full Text](#)
26. Schmittgen TD, Livak KJ: **Analyzing real-time PCR data by the comparative C_t method.** *Nat Protoc.* 2008; 3(6): 1101–1108.
[PubMed Abstract](#) | [Publisher Full Text](#)
27. Yazawa, M, Hsueh B, Jia X, *et al.*: **Using induced pluripotent stem cells to investigate cardiac phenotypes in Timothy syndrome.** *Nature.* 2011; 471(7337): 230–4.
[PubMed Abstract](#) | [Publisher Full Text](#) | [Free Full Text](#)
28. Kondrashov A, Duc Hoang M, Smith JGW, *et al.*: **Simplified Footprint-Free Cas9/CRISPR Editing of Cardiac-Associated Genes in Human Pluripotent Stem Cells.** *Stem Cells Dev.* 2018; 27(6): 391–404.
[PubMed Abstract](#) | [Publisher Full Text](#) | [Free Full Text](#)
29. Sala L, Bellin M, Mummery CL: **Integrating cardiomyocytes from human pluripotent stem cells in safety pharmacology: Has the time come?** *Br J Pharmacol.* 2017; 174(21): 3749–3765.
[PubMed Abstract](#) | [Publisher Full Text](#) | [Free Full Text](#)
30. Eckersley-Maslin MA, Spector DL: **Random monoallelic expression: regulating gene expression one allele at a time.** *Trends Genet.* 2014; 30(6): 237–44.
[PubMed Abstract](#) | [Publisher Full Text](#) | [Free Full Text](#)
31. Luo Y, Liu C, Cerbini T, *et al.*: **Stable enhanced green fluorescent protein expression after differentiation and transplantation of reporter human induced pluripotent stem cells generated by AAVS1 transcription activator-like effector nucleases.** *Stem Cells Transl Med.* 2014; 3(7): 821–35.
[PubMed Abstract](#) | [Publisher Full Text](#) | [Free Full Text](#)
32. Kim JH, Lee SR, Li LH, *et al.*: **High cleavage efficiency of a 2A peptide derived from porcine teschovirus-1 in human cell lines, zebrafish and mice.** *PLoS One.* 2011; 6(4): e18556.
[PubMed Abstract](#) | [Publisher Full Text](#) | [Free Full Text](#)

Open Peer Review

Current Peer Review Status:



Version 2

Reviewer Report 30 July 2020

<https://doi.org/10.5256/f1000research.26839.r67081>

© 2020 Howden S. This is an open access peer review report distributed under the terms of the [Creative Commons Attribution License](#), which permits unrestricted use, distribution, and reproduction in any medium, provided the original work is properly cited.



Sara Howden

Murdoch Children's Research Institute (MCRI), Melbourne, Vic, Australia

In this study, the authors clearly show that targeting transgenes to the "safe harbour" AAVS1 results in highly variable transgene expression in iPSCs, which is exacerbated even further following differentiation. This has important implications for researchers contemplating this locus for generating iPSC lines to stably express a transgene of interest (e.g fluorescent reporter, Cas9, transcription factor etc) The study appears well executed and their conclusions are well supported by their findings. One minor comment but certainly not a deal breaker, it would have been nice to see clones analysed by flow cytometry. This would not only give a very accurate picture of the number of cells expressing the given reporter but also a more accurate picture of the level of transgene expression (i.e median peak fluorescence) not only between clones but within clones.

Also, might be helpful if the authors indicate how they separate endogenous HOXA9 expression from exogenous (transgene) expression.

All in all, a great little study with very useful data/implications for those in the field!

Is the work clearly and accurately presented and does it cite the current literature?

Yes

Is the study design appropriate and is the work technically sound?

Yes

Are sufficient details of methods and analysis provided to allow replication by others?

Partly

If applicable, is the statistical analysis and its interpretation appropriate?

I cannot comment. A qualified statistician is required.

Are all the source data underlying the results available to ensure full reproducibility?

Yes

Are the conclusions drawn adequately supported by the results?

Yes

Competing Interests: No competing interests were disclosed.

Reviewer Expertise: Gene editing, pluripotent stem cells, kidney differentiation

I confirm that I have read this submission and believe that I have an appropriate level of expertise to confirm that it is of an acceptable scientific standard.

Reviewer Report 10 July 2020

<https://doi.org/10.5256/f1000research.26839.r66913>

© 2020 Carr C. This is an open access peer review report distributed under the terms of the [Creative Commons Attribution License](#), which permits unrestricted use, distribution, and reproduction in any medium, provided the original work is properly cited.



Carolyn Carr 

Department of Physiology, Anatomy and Genetics, University of Oxford, Oxford, UK

No further comments

Is the work clearly and accurately presented and does it cite the current literature?

Yes

Is the study design appropriate and is the work technically sound?

Yes

Are sufficient details of methods and analysis provided to allow replication by others?

Yes

If applicable, is the statistical analysis and its interpretation appropriate?

Yes

Are all the source data underlying the results available to ensure full reproducibility?

Yes

Are the conclusions drawn adequately supported by the results?

Yes

Competing Interests: No competing interests were disclosed.

Reviewer Expertise: Cardiac physiology and cardiac stem cells for regeneration, disease phenotyping and drug testing

I confirm that I have read this submission and believe that I have an appropriate level of expertise to confirm that it is of an acceptable scientific standard.

Version 1

Reviewer Report 23 March 2020

<https://doi.org/10.5256/f1000research.21830.r61069>

© 2020 Verfaillie C et al. This is an open access peer review report distributed under the terms of the [Creative Commons Attribution License](#), which permits unrestricted use, distribution, and reproduction in any medium, provided the original work is properly cited.

**Catherine M. Verfaillie** 

Stem Cell Institute Leuven, Department of Development and Regeneration, KU Leuven, Leuven, Belgium
Yannan Fan

KU Leuven, Leuven, Belgium

In this paper, the authors aim to investigate the effect of hypertrophic cardiomyopathy associated mutations *MYH7C*^{G123T} and *ACTC1*^{G301A} on Ca²⁺ transients using hiPSCs- derived cardiomyocytes. To this end, the authors established hiPSCs reporters by introducing a CAG promotor-controlled calcium indicator (R-GECO1.0) into the *AAVS1* locus through CRISPR/Cas9 nickase-mediated genome editing. Among 24 clones, 20 were found to successfully express the transgene with variation from about 0 to 99.5%. Upon differentiation to cardiomyocytes, even clones with high expression levels demonstrated significant silencing of the transgene to 13.03% or 1.33%. By creating also an *AAVS1* targeted doxycycline inducible HOXA9-T2A-mScarlet iPSCs reporter, the authors investigated the silencing over the time course during mesoderm lineage commitment. It was shown that both mRNA and protein levels of the transgenes were relatively high on day 2 and abruptly decreased from day 4 during both cardiomyocyte and hematopoietic differentiation.

Despite the silencing of R-GECO1.0 in the *AAVS1* locus, Ca²⁺ live image by confocal laser line scan microscopy at the single cell level detected abnormal Ca²⁺ transients in cardiomyocytes derived from hiPSCs reporters harboring *MYH7C* or *ACTC1* mutations compared to wildtype or isogenic control. In addition, this abnormality could be rescued by pharmacological inhibiting intercellular level of Na⁺ and Ca²⁺.

This study shows that iPSC reporter line is of importance for disease modelling. This study presented an important issue in *AAVS1*-targeted transgene expression in iPSCs and mesoderm lineage although the mechanisms for the silencing are not clear. The variable expression and silencing in mesoderm differentiation shown here are in line with previous reports that the *AAVS1* is not a true safe harbor for cells differentiated to hematopoietic cells (e.g. PMID: 31773990) and endoderm (e.g. PMID: 26455413); and, hence, the findings are not fully novel.

Specific comments:

1. The authors did not mention why for they compared wild-type (*MYH7*^{WT/WT}), heterozygous (*MYH7*^{WT/MUT}) and homozygous (*MYH7*^{MUT/MUT}) for the c.*MYH7*^{C9123T} mutation, but no homozygous mutant line for *ACTC1*^{G301A}.
2. In Fig 2A, the expression of R-GECO in *ACTC1*^{WT/MUT} clones (1/5 with about 50% cells) was lower than in *ACTC1*^{WT/WT} clones. Is this chance or due to the mutation?

3. In Fig 2A, it would be better to show R-GECO in red and OCT4 in green to retain consistency with other images.
4. In Fig 3C, immunostaining in the upper images showed R-GECO in red while in the lower ones R-GECO is stained in green, which is difficult to follow.
5. It is interesting to see that puromycin enrichment of the iPSCs over 3 passages increased R-GECO1.0 expression in *MYH7*^{MUT/MUT} 15, did the author also tried puromycin enrichment in *MYH7*^{WT/MUT}?
6. In the introduction, the authors mention that a doxycycline-inducible HOXA9-T2A-mScarlet cassette targeted in the *AAVS1* locus of hiPSCs is used for modulating HOXA9 during hematopoietic differentiation. However, this iPSC reporter is also used for cardiomyocyte differentiation (Fig 4A). It is unclear whether there is specific reason why this reporter line is used instead of *AAVS1*-CAG R-GECO iPSCs.
7. It is better to present RTqPCR result using a Δ Ct method for Fig. 4 as fold changes are confusing especially in the context of transgene expression (the biological relevance of fold change is unclear unless one knows the base line transcript levels before gene activation).
8. In Fig 6 - Western Blot (Extended data), to test the peptide cleavage of P2A and T2A, the authors state that P2A is less efficient than T2A, as NpHR expression (following a P2A) was barely visible. The authors should provide positive control to exclude that the antibody for NpHR did not work.
9. Southern blots should be performed to make sure that clones tested in this study were targeted in the corrected locus, and silencing was not due to random integration.

Is the work clearly and accurately presented and does it cite the current literature?

Partly

Is the study design appropriate and is the work technically sound?

Yes

Are sufficient details of methods and analysis provided to allow replication by others?

Yes

If applicable, is the statistical analysis and its interpretation appropriate?

Yes

Are all the source data underlying the results available to ensure full reproducibility?

Yes

Are the conclusions drawn adequately supported by the results?

Partly

Competing Interests: No competing interests were disclosed.

Reviewer Expertise: iPSC, differentiation, genome editing

We confirm that we have read this submission and believe that we have an appropriate level of expertise to state that we do not consider it to be of an acceptable scientific standard, for reasons outlined above.

Author Response 21 May 2020

Jamie Bhagwan, University of Nottingham, Nottingham, UK

Dear Reviewer,

Thank you for your comments on our manuscript entitled *Variable expression and silencing of CRISPR-Cas9 targeted transgenes identifies the AAVS1 locus as not an entirely safe harbour*.

We have endeavoured to respond to your comments and suggestions as outlined below in bold font.

In this paper, the authors aim to investigate the effect of hypertrophic cardiomyopathy associated mutations *MYH7C*^{G123T} and *ACTC1*^{G301A} on Ca²⁺ transients using hiPSCs- derived cardiomyocytes.

To this end, the authors established hiPSCs reporters by introducing a CAG promotor-controlled calcium indicator (R-GECO1.0) into the *AAVS1* locus through CRISPR/Cas9 nickase-mediated genome editing. Among 24 clones, 20 were found to successfully express the transgene with variation from about 0 to 99.5%. Upon differentiation to cardiomyocytes, even clones with high expression levels demonstrated significant silencing of the transgene to 13.03% or 1.33%. By creating also an *AAVS1* targeted doxycycline inducible HOXA9-T2A-mScarlet iPSCs reporter, the authors investigated the silencing over the time course during mesoderm lineage commitment. It was shown that both mRNA and protein levels of the transgenes were relatively high on day 2 and abruptly decreased from day 4 during both cardiomyocyte and hematopoietic differentiation. Despite the silencing of R-GECO1.0 in the *AAVS1* locus, Ca²⁺ live image by confocal laser line scan microscopy at the single cell level detected abnormal Ca²⁺ transients in cardiomyocytes derived from hiPSCs reporters harboring *MYH7C* or *ACTC1* mutations compared to wildtype or isogenic control. In addition, this abnormality could be rescued by pharmacological inhibiting intercellular level of Na⁺ and Ca²⁺.

This study shows that iPSC reporter line is of importance for disease modelling. This study presented an important issue in *AAVS1*-targeted transgene expression in iPSCs and mesoderm lineage although the mechanisms for the silencing are not clear. The variable expression and silencing in mesoderm differentiation shown here are in line with previous reports that the *AAVS1* is not a true safe harbor for cells differentiated to hematopoietic cells (e.g. PMID: 31773990) and endoderm (e.g. PMID: 26455413); and, hence, the findings are not fully novel.

We note the reviewer's comments regarding novelty of the findings. However, the Klatt *et al.* paper (PMID: 31773990) was published after the submission of this manuscript. The Klatt *et al.* paper was first published online on 27 November 2019, whilst this manuscript was first published on 12 November 2019, so the variable expression and silencing upon hematopoietic differentiation was undocumented prior to the submission of this manuscript. Nonetheless, the Klatt *et al.* paper adds weight to the notion of *AAVS1* silencing, and elegantly demonstrates the contextual methylation of *AAVS1*-targeted transgenes depending on the promoter inserted into the site. We also note the Luo *et al.* 2014 paper (PMID: 24833591) which showed silencing of eGFP expression at the *AAVS1*

site when using the EF1 α promoter that was overcome by replacing it with the CAG promoter. Indeed, this paper informed our choice of promoter for the RGECO targeting construct.

The penultimate sentence of the third paragraph in the Introduction now reads:

“However, some reports of DNA methylation dampening transgene expression in both hPSC-derived hepatocytes (Ordovás *et al.*, 2015) and iPSC-derived myeloid progenitors (Klatt *et al.*, 2020) raise questions on whether a ‘perfect’ safe harbour locus exists”

The Discussion now reads:

“Transgene silencing at the AAVS1 locus has previously been shown upon differentiation towards hepatocyte-like cells, with de novo methylation of the locus found to be responsible (Ordovás *et al.*, 2015). However, the aforementioned report claims that this silencing effect is restricted to endoderm differentiations. With the use of the AAVS1-targeted HOXA9-T2A-mScarlet cell line, we show that in two mesoderm-specific differentiations towards cardiomyocytes and haematopoietic cells, silencing of expression occurs immediately after mesoderm specification and peak expression of *MIXL1* and *Brachyury*. This is in agreement with a recent report which demonstrated differential transgene methylation in AAVS1-targeted iPSC-derived myeloid cells (Klatt *et al.*, 2020).”

And

“Indeed, the CAG promoter appears to exhibit some insulation from methylation of transgenes at the AAVS1 locus (Ordovás *et al.*, 2015). In addition, a recent report elegantly demonstrated that contextual silencing at the AAVS1 locus of iPSC-derived myeloid precursors can occur with varying efficiency depending on the chosen promoter (Klatt *et al.*, 2020).”

The authors recognise and acknowledge that this phenomenon has been shown in endoderm and this is referred to in the manuscript.

The last paragraph of the Introduction contains the following sentence:

“This suggests that silencing at the AAVS1 locus is not limited to the endoderm lineage as previously described (Ordovás *et al.*, 2015).

The Discussion states that:

“Our results dispute the claims of robust and persistent transgene expression from AAVS1, and complements reports that show silencing at AAVS1 upon differentiation to endoderm lineage (Ordovás *et al.*, 2015)”

Specific comments:

1. The authors did not mention why for they compared wild-type (*MYH7*^{WT/WT}), heterozygous (*MYH7*^{WT/MUT}) and homozygous (*MYH7*^{MUT/MUT}) for the c.*MYH7*^{C9123T} mutation, but no homozygous mutant line for *ACTC1*^{G301A}. **The authors apologise for not making this**

clearer in the text. The discrepancy between the range of genetically-engineered lines exhibiting the *MYH7*- or *ACTC1*- mutations is due to the source of the cells and their subsequent CRISPR/Cas9 targeting strategy. The *MYH7*-mutant hiPSC lines were generated by targeting the WT allele of unrelated healthy cell lines or origin (Mosqueira *et al.*, 2018), enabling the generation of heterozygous and homozygous clones. In contrast, the isogenic set of *ACTC1* lines was generated by genomic correction of the mutant allele of the starting hiPSC line derived from a heterozygous patient (using a donor vector containing the WT allele only) (Smith *et al.*, 2018, Kondrashov *et al.*, 2018). As such, homozygous mutant clones could not be generated by employing this strategy. Notwithstanding, the vast majority of HCM-causing mutations in the sarcomeric genes are heterozygous (Lopes *et al.*, 2013), as homozygous mutations tend to be lethal. In particular, the mutations under study (p.R453C- β MHC and p.E99K-*ACTC1*) have never reported to be homozygous in patients, to the best of our knowledge. Therefore, the cellular models generated already encompass the patient-relevant genotypic status and as such provide an accurate characterization of HCM *in vitro*. Homozygous mutant lines were included to provide extra readout sensitivity for the phenotypic assays developed (as seen by more severe phenotypes in Figure 5). The first paragraph of the Results section now reads: “Our overarching goal was to create two isogenic sets of hiPSC lines in order to study Ca^{2+} handling in the context of *in vitro* models of the disease HCM. One isogenic trio comprised lines that were originally wild-type (*MYH7*^{WT/WT}) and then CRISPR Cas9 edited to generate heterozygous (*MYH7*^{WT/MUT}) and homozygous (*MYH7*^{MUT/MUT}) mutants for the c. *MYH7*^{C9123T} mutation (Mosqueira *et al.*, 2018). The other comprised a pair that were originally patient-derived heterozygous (*ACTC1*^{WT/MUT}) for the c. *ACTC1*^{G301A} mutation and CRISPR Cas9 corrected (*ACTC1*^{WT/WT}) (Smith *et al.*, 2018, Kondrashov *et al.*, 2018).

2. In Fig 2A, the expression of R-GECO in *ACTC1*^{WT/MUT} clones (1/5 with about 50% cells) was lower than in *ACTC1*^{WT/WT} clones. Is this chance or due to the mutation? **We believe that this is unlikely to be due to the ACTC1 mutation but simply highlights the variability between different cell lines. Each cell line, and subsequently, each clone seemingly has varying levels of transgene silencing and extensive screening is therefore required, as we have performed.**
3. In Fig 2A, it would be better to show R-GECO in red and OCT4 in green to retain consistency with other images. **Agreed. The images in Figure 2A for *MYH7*^{MUT/MUT} clone 1 and *MYH7*^{MUT/MUT} clone 4 have now been pseudocoloured to match the other images in the panel.**
4. In Fig 3C, immunostaining in the upper images showed R-GECO in red while in the lower ones R-GECO is stained in green, which is difficult to follow. **Agreed. To retain consistency, the upper images in Figure 3C have been pseudocoloured so that R-GECO is always represented as red. Figure 2D and all accompanying graphs have also been changed to aid consistency.**
5. It is interesting to see that puromycin enrichment of the iPSCs over 3 passages increased R-GECO1.0 expression in *MYH7*^{MUT/MUT} 15, did the author also tried puromycin enrichment in *MYH7*^{WT/MUT}? **Our aim was to have a high enough percentage of cardiomyocytes expressing R-GECO so that confocal line scan analysis was technically feasible. The *MYH7*^{MUT/MUT} 15 clone was originally enriched due to the extremely low level of cardiomyocyte R-GECO expression making it difficult to**

perform single cell analysis. In contrast, the 13.03% R-GECO expression in the *MYH7*^{WT/MUT} clone was sufficient to find R-GECO expressing cardiomyocytes in a single field of view. Therefore, antibiotic selection of the *MYH7*^{WT/MUT} line was not necessary. The purpose of Figure 3D is to provide a technical solution to lower levels or R-GECO expression, when required.

6. In the introduction, the authors mention that a doxycycline-inducible HOXA9-T2A-mScarlet cassette targeted in the *AAVS1* locus of hiPSCs is used for modulating HOXA9 during hematopoietic differentiation. However, this iPSC reporter is also used for cardiomyocyte differentiation (Fig 4A). It is unclear whether there is specific reason why this reporter line is used instead of *AAVS1*-CAG R-GECO iPSCs. **We acknowledge the Reviewer's point. As cardiomyocyte and haematopoietic differentiation share developmental stages (e.g., mesoderm induction), and given that HOXA9 was also shown to be expressed in early cardiac progenitor cells of the cardiac crescent (Behrens et al., 2013), we opted to perform both cardiomyocyte and haematopoietic differentiations using the HOXA9-T2A-mScarlet line. The introduction has been amended to clarify the overall purpose of the HOXA9-T2A-mScarlet line:**

"In addition, CRISPR Cas9 targeting of the *AAVS1* locus was used to target a doxycycline-inducible HOXA9-T2A-mScarlet cassette into hiPSCs. HOXA9 is a transcription factor regulated spatio-temporally during haematopoietic or cardiac development (Behrens *et al.*, 2013) and the aim was to examine if controlled supplemental expression of HOXA9 resulted in more efficient production of mature cells."

1. It is better to present RTqPCR result using a Δ Ct method for Fig. 4 as fold changes are confusing especially in the context of transgene expression (the biological relevance of fold change is unclear unless one knows the base line transcript levels before gene activation). **We believe that the $\Delta\Delta$ Ct method gives a better visualisation of the changes in transgene expression. The data in Figure 4 is presented as relative expression compared to *untargeted* iPSCs. Nevertheless, graphical presentation of Δ Ct values are provided in Extended data (Figure 9 Delta Ct representation of HOXA9 expression in *AAVS1*-targeted hiPSCs).**
2. In Fig 6 - Western Blot (Extended data), to test the peptide cleavage of P2A and T2A, the authors state that P2A is less efficient than T2A, as NpHR expression (following a P2A) was barely visible. The authors should provide positive control to exclude that the antibody for NpHR did not work. **While the authors agree that this could enhance the data, our initial assessment was based on the 60kDa protein being, in all likelihood, a fusion of Chr2 (30kDa) and NpHR (30kDa). The anti-eNpHR antibody (catalog #AS12 1851; Agrisera) has been validated for use in Western Blot applications but unfortunately is not provided with a positive control sample.**
3. Southern blots should be performed to make sure that clones tested in this study were targeted in the corrected locus, and silencing was not due to random integration. **The authors agree that integration of the cassette into the *AAVS1* locus is vital. This was tested using PCR genotyping from outside the arms of homology and into the cassette as shown in Figure 1. As an alternative to southern blots, we have now included original PCR screening gels as extended data (Figure 7 – PCR screening of hiPSC clones to check for *AAVS1* integration). In addition, we have included details of the sgRNA design (Figure 8 – sgRNA design) and show that all off-target locations occur in introns (Table 2.1 Guide 2 off-targets and Table 2.2 Guide 3 off-targets).**

References

Behrens AN, Iacovino M, Lohr JL, et al.: Nkx2-5 mediates differential cardiac differentiation through interaction with Hoxa10. *Stem Cells Dev.* 2013;22(15):2211-2220. 23477547 10.1089/scd.2012.0611

Klatt D, Cheng E, Hoffmann D, et al.: Differential Transgene Silencing of Myeloid-Specific Promoters in the AAVS1 Safe Harbor Locus of Induced Pluripotent Stem Cell-Derived Myeloid Cells. *Hum Gene Ther.* 2020;31(3-4):199-210. 31773990 10.1089/hum.2019.194

Kondrashov A, Duc Hoang M, Smith JGW, et al.: Simplified Footprint-Free Cas9/CRISPR Editing of Cardiac-Associated Genes in Human Pluripotent Stem Cells. *Stem Cells Development.* 2018;27(6):391-404. 29402189 10.1089/scd.2017.0268 5882176

Lopes LR, Zekaviti A, Syrris P, et al.: Genetic Complexity in Hypertrophic Cardiomyopathy Revealed by High Throughput Sequencing. *J Med Genet.* 2013;50(4):228-39. 23396983 10.1136/jmedgenet-2012-101270

Luo Y, Liu C, Cerbini T, et al.: Stable enhanced green fluorescent protein expression after differentiation and transplantation of reporter human induced pluripotent stem cells generated by AAVS1 transcription activator-like effector nucleases. *Stem Cells Transl Med.* 2014;3(7):821-35. 24833591 10.5966/sctm.2013-0212 4073825

Mosqueira D, Mannhardt I, Bhagwan JR, et al.: CRISPR/Cas9 editing in human pluripotent stem cell-cardiomyocytes highlights arrhythmias, hypocontractility, and energy depletion as potential therapeutic targets for hypertrophic cardiomyopathy. *Eur Heart J.* 2018;39(43):3879-3892. 29741611 10.1093/eurheartj/ehy249 6234851

Ordovás L, Boon R, Pistoni M, et al.: Efficient Recombinase-Mediated Cassette Exchange in hPSCs to Study the Hepatocyte Lineage Reveals AAVS1 Locus-Mediated Transgene Inhibition. *Stem Cell Reports.* 2015;5(5):918-31. 26455413 10.1016/j.stemcr.2015.09.004 4649136

Smith JGW, Owen T, Bhagwan JR, et al.: Isogenic Pairs of hiPSC-CMs with Hypertrophic Cardiomyopathy/LVNC-Associated ACTC1 E99K Mutation Unveil Differential Functional Deficits. *Stem Cell Reports.* 2018;11(5):1226-1243. 30392975 10.1016/j.stemcr.2018.10.006 6235010

Competing Interests: No competing interests were disclosed.

Reviewer Report 29 November 2019

<https://doi.org/10.5256/f1000research.21830.r56469>

© 2019 Carr C. This is an open access peer review report distributed under the terms of the [Creative Commons Attribution License](#), which permits unrestricted use, distribution, and reproduction in any medium, provided the original work is properly cited.



Carolyn Carr 

Department of Physiology, Anatomy and Genetics, University of Oxford, Oxford, UK

There are two arms to this manuscript. The authors aimed to determine the reliability of introducing a transgene containing a calcium indicator (R-GECO1.0) or a fluorescent reporter (HOXA9-T2A-mScarlet) into the AAVS1 locus using CRISPR-Cas9 and then subsequently investigate the effect of mutations in *MYH7* or *ACTC1* on calcium handling.

Initial experiments showed that although the AAVS1 could be targeted successfully in 20/24 clones, the expression of the transgene was highly variable. Furthermore, on differentiation of the more successfully transfected clones to cardiomyocytes, the transgene was silenced with almost complete removal of expression of the fluorescent reporter. A similar degree of silencing was observed during haematopoietic differentiation.

Using the mScarlet reporter the authors investigated the timecourse of downregulation and found that with both cardiomyocyte and haematopoietic differentiation, increased transgene expression was observed at day 2 but then decreased substantially over time, at both the mRNA and protein level.

Nevertheless, using puromycin selection, it was possible to isolate single cardiomyocytes expressing the R-GECO reporter and these were used to show that mutations in both *MYH7* and *ACTC1* resulted in abnormal calcium transient events which could be corrected in part using ranolazine and dantrolene.

This is a valuable piece of work which demonstrates shortfalls in what was expected to be a fairly reliable transfection protocol and that the AAVS1 locus is not as foolproof a site for transfection as may have been thought. The addition of the calcium transient measurements is interesting in that it shows that something can be rescued from such a large body of work, but it does come as rather an afterthought in the manuscript.

I have a few minor comments to aid clarity:

- The introduction needs to be expanded somewhat. The paragraph on modulating HOXA9 is very brief and the rationale needs to be explained. In the results section this appears to be merely a way of monitoring transgene expression, but the short paragraph in the introduction implies some sort of mechanistic approach.
- It is not entirely clear to me what the difference is between the data shown in Fig 2D and 3B apart from different clones.
- In the section on HOXA9-T2A targeting it says in results that doxycycline was administered every 48 hours. This is not mentioned in the methods or the extended information. The authors state that transgene induction decreased after day 2. Was this reduction despite further addition of doxycycline?
- In figure 5, the timing on the x axis is given in parts H and I but not in other plots. In some others there is a bar but this is not explained. Is the scale the same throughout? If so, some comment should be made as to why the wild type MYH7 cells have a slower beat rate than the ACTC1 wild type cells. The same formatting should be used on all the graphs.

Is the work clearly and accurately presented and does it cite the current literature?

Yes

Is the study design appropriate and is the work technically sound?

Yes

Are sufficient details of methods and analysis provided to allow replication by others?

Partly

If applicable, is the statistical analysis and its interpretation appropriate?

Yes

Are all the source data underlying the results available to ensure full reproducibility?

Yes

Are the conclusions drawn adequately supported by the results?

Yes

Competing Interests: No competing interests were disclosed.

Reviewer Expertise: Cardiac physiology and cardiac stem cells for regeneration, disease phenotyping and drug testing.

I confirm that I have read this submission and believe that I have an appropriate level of expertise to confirm that it is of an acceptable scientific standard.

Author Response 21 May 2020

Jamie Bhagwan, University of Nottingham, Nottingham, UK

Dear Reviewer,

Thank you for your comments on our manuscript entitled *Variable expression and silencing of CRISPR-Cas9 targeted transgenes identifies the AAVS1 locus as not an entirely safe harbour*.

We have endeavoured to respond to your comments and suggestions as outlined below in bold font.

There are two arms to this manuscript. The authors aimed to determine the reliability of introducing a transgene containing a calcium indicator (R-GECO1.0) or a fluorescent reporter (HOXA9-T2A-mScarlet) into the AAVS1 locus using CRISPR-Cas9 and then subsequently investigate the effect of mutations in *MYH7* or *ACTC1* on calcium handling.

Initial experiments showed that although the AAVS1 could be targeted successfully in 20/24 clones, the expression of the transgene was highly variable. Furthermore, on differentiation of the more successfully transfected clones to cardiomyocytes, the transgene was silenced with almost complete removal of expression of the fluorescent reporter. A similar degree of silencing was observed during haematopoietic differentiation.

Using the mScarlet reporter the authors investigated the timecourse of downregulation and found that with both cardiomyocyte and haematopoietic differentiation, increased transgene expression was observed at day 2 but then decreased substantially over time, at both the mRNA and protein level.

Nevertheless, using puromycin selection, it was possible to isolate single cardiomyocytes expressing the R-GECO reporter and these were used to show that mutations in both *MYH7* and *ACTC1* resulted in abnormal calcium transient events which could be corrected in part using ranolazine and dantrolene.

This is a valuable piece of work which demonstrates shortfalls in what was expected to be a fairly

reliable transfection protocol and that the AAVS1 locus is not as foolproof a site for transfection as may have been thought. The addition of the calcium transient measurements is interesting in that it shows that something can be rescued from such a large body of work, but it does come as rather an afterthought in the manuscript.

I have a few minor comments to aid clarity:

- The introduction needs to be expanded somewhat. The paragraph on modulating HOXA9 is very brief and the rationale needs to be explained. In the results section this appears to be merely a way of monitoring transgene expression, but the short paragraph in the introduction implies some sort of mechanistic approach.

For the purposes of this paper the HOXA9 model is simply used a tool to monitor transgene expression. However, its overall purpose in the context of haematopoiesis is now described in the introduction for completeness. The penultimate paragraph of the Introduction now reads:

“In addition, CRISPR Cas9 targeting of the AAVS1 locus was used to target a doxycycline-inducible HOXA9-T2A-mScarlet cassette into hiPSCs. HOXA9 is a transcription factor regulated spatio-temporally during haematopoietic or cardiac development (Behrens *et al.*, 2013) and the aim was to examine if controlled supplemental expression of HOXA9 resulted in more efficient production of mature cells.”

- It is not entirely clear to me what the difference is between the data shown in Fig 2D and 3B apart from different clones.

Yes, we concede that these experiments are similar. However, Fig 2D is intended to show variability within an isogenic set of clones differentiated to cardiomyocytes, whereas Fig 3B is intended as a comparison between isogenic sets of clones and complements the data in Fig 3A.

- In the section on HOXA9-T2A targeting it says in results that doxycycline was administered every 48 hours. This is not mentioned in the methods or the extended information. The authors state that transgene induction decreased after day 2. Was this reduction despite further addition of doxycycline?

Yes, this reduction did occur despite further addition of doxycycline every 2 days. In addition to text in the results and the figure legend for Figure 3, the methods have now been clarified with a sentence in the ‘Live imaging of mScarlet’ section which now reads:

“HOXA9 and mScarlet expression was induced with the addition of 1 µg/ml doxycycline every 48 hours.”

- In figure 5, the timing on the x axis is given in parts H and I but not in other plots. In some others there is a bar but this is not explained. Is the scale the same throughout? If so, some comment should be made as to why the wild type MYH7 cells have a slower beat rate than the ACTC1 wild type cells. The same formatting should be used on all the graphs.

The authors apologise for the error. The x axis scale bar relates to time (5 seconds) and the y-axis scale bar relates to the length of the laser line drawn across the cell to perform the confocal line scan. All panels now contain both scale bars and the legend for Figure 5 has been corrected to include this information. The methods have also been clarified to state that these line scans are performed on spontaneously beating cardiomyocytes, hence their slightly varied beat rate. The

end of the first paragraph of the ‘confocal analysis’ methods sections now reads:

“Line-scan images were taken every 75 milliseconds, with a pixel dwell time of 4.12 μ sec, for a total of 4000 cycles resulting in a five minute scan. CMs were kept at 37°C and 5% CO₂ and allowed to spontaneously beat throughout data acquisition.”

Differences in beat rate and action potential duration between healthy hiPSC-CMs are common, as previously reviewed (Sala *et al.*, 2017). This further advocates the need for isogenic lines in order to ensure that the impact of the mutation studied is accurately investigated. The fourth sentence of the section entitled

“AAVS1-targeted R-GECO1.0 expressing clones as a tool for in vitro disease modelling and drug screening” now reads:

“Despite some expected variability in spontaneous beat rate between wild-type hiPSC-CMs (Figure 5A and 5E) (Sala *et al.*, 2017), for both the c. *MYH7* C9123T and c. *ACTC1* G301A mutations, increasing mutation load resulted in an increased incidence of abnormal Ca²⁺ transient events.”

References

Behrens AN, Iacovino M, Lohr JL, et al.: Nkx2-5 mediates differential cardiac differentiation through interaction with Hoxa10. *Stem Cells Dev.* 2013;22(15):2211-2220. 23477547
10.1089/scd.2012.0611

Sala L, Bellin M, Mummery CL.: Integrating cardiomyocytes from human pluripotent stem cells in safety pharmacology: Has the time come? *Br J Pharmacol.* 2017;174(21):3749-3765. 27641943
10.1111/bph.13577

Competing Interests: No competing interests were disclosed.

The benefits of publishing with F1000Research:

- Your article is published within days, with no editorial bias
- You can publish traditional articles, null/negative results, case reports, data notes and more
- The peer review process is transparent and collaborative
- Your article is indexed in PubMed after passing peer review
- Dedicated customer support at every stage

For pre-submission enquiries, contact research@f1000.com

F1000Research